

THE INFLUENCE OF HYPORHEIC FLOW ON STREAM TEMPERATURE
CHANGE AND HEAT ENERGY BUDGET IN HEADWATER RIFFLE-STEP-
POOL STREAM IN THE BOISE FRONT, IDAHO

by

Eric Louis Rothwell

A thesis

submitted in partial fulfillment of the

requirements for the degree of

Master of Science in Geology

Boise State University

January, 2005

The thesis presented by Eric L. Rothwell entitled The Stream Temperature And The Influence Of Hyporheic Flow On Stream Temperature Change And Heat Energy Budget In Headwater Riffle-Step-Pool Stream In The Boise Front, Idaho is hereby approved:

Advisor

Date

Committee Member

Date

Committee Member

Date

Graduate Dean

Date

Dedication page

Acknowledgements

ABSTRACT

TABLE OF CONTENTS

1. INTRODUCTION

1.3 Overview

The federal Clean Water Act, National Environmental Policy Act and Endangered Species Act require knowledge of parameters controlling water and stream quality. Stream temperature, both daily and seasonally, can arguably be the most important control on all life processes in streams; temperature influences growth rates, life cycles and productivity. Consequently, stream temperature is often used as an indicator of watershed health and watershed managers are commonly asked to assess the potential impacts of land-use practices on stream temperature; understanding the process of stream temperature change is particularly important during summer months when stream temperature peaks are correlated with long days, high air temperature and low stream flow.

Stream temperature is controlled by energy fluxes into and out of a stream. Predicting stream temperature is complicated by the spatial and temporal variability of energy fluxes interacting with the stream that control stream temperature. The most rigorous physically based approach to evaluate stream temperature change is by using conservation of energy in a heat-energy budget, referred to as a heat budget for the remainder of this text. By applying mass and energy conservation in a heat budget model stream temperature can be accurately predicted. The heat-energy budget approach is greatly improved with the advancements in the meteorological equipment as well as the ability for this equipment to be installed in or adjacent to the stream. Positive heat fluxes, those that go into a stream, dominated by solar and short wave radiation (net

radiation), sensible heat exchange with the atmosphere and advection of heat by transfer of water into and out of the stream. Losing heat fluxes that buffer stream temperature and may provide cooling are dominated by bed conduction, evaporation and advection of water. Failures of the heat budget approach to modeling stream temperature are often due to inadequate representation of all the processes that control stream temperature.

To better predict temperature change a hyporheic flow component is included in the heat budget. Hyporheic flow is the advection of stream water through and interacting with underlying sediment, bedrock and groundwater and returning to the stream. Hyporheic flow, driven by gradient and controlled by morphology and substrate properties, influences stream temperature by temporarily removing water from the heating impact of solar radiation and other positive heat fluxes at the surface of the stream and returning flow from the substrate out of phase with stream temperature. The heat budget is analyzed to assess the impact of neglecting hyporheic flow on the prediction of downstream temperature changes.

1.2 Problem Statement

The most rigorous understanding of stream temperature change is achieved by a heat budget approach; failures of the heat budget approach to modeling stream temperature are often due to inadequate representation of all the processes that control stream temperature. In order to understand processes controlling stream temperature a heat budget model is used with all relevant energy flux components. There have been few studies that incorporate the influence of hyporheic flow on heat budgets and stream temperature.

1.3 Purpose and Objectives

The ability to predict stream temperature is important due to the many direct and indirect water use and watershed management effects on streams. Predicting temperature change over a short reach by using a heat energy budget provides an understanding of stream processes influence on stream temperature. By including the influence of hyporheic flow in a stream heat budget we gain knowledge of hyporheic flow in terms of absolute heat flux and relative importance compared to other major heat fluxes (i.e. net radiation, evaporation etc.) and their influence on stream temperature change. This provides an indirect measure of the importance of stream morphology. Stream temperature models can be used as a tool to quantify ecosystem health, environmental rehabilitation success or as a degradation indicator.

In this study I evaluate the impact of hyporheic flow on a heat budget approach to predict downstream changes in stream temperature. The overall goal of this study is to increase the understanding of the flow-paths of energy and water in a small stream. With in this goal I hope to:

- Accurately predict longitudinal temperature change in stream waters by using a heat budget model.
- Assess the relative importance of heat budget components.
- And evaluate the impact of neglecting hyporheic flow in an energy budget approach to predict downstream changes in stream temperature.

1.4 Background

1.4.1 Stream temperature and ecological effects

Stream temperature is generally raised by human activity in a watershed due to impoundment of flow, decrease in flow by diversion, stream alterations and reduction in shading near the stream. All stream organisms are restricted by thermal conditions of the stream water. Timing of life cycles for various aquatic species are cued and regulated by temperature; temperature also regulates growth rates and productivity (Allen, 2001). With higher temperatures the solubility of oxygen decreases. Higher stream temperatures increasing the metabolism of aquatic species and the increase in metabolism respiration compound the depletion of dissolved oxygen, and so the oxygen demand increases as well (McKee and Wolf, 1963). With an increase in stream temperature and growth rate the incident of disease and may increase (Rucker et al., 1953; Allen, 2001).

1.4.2 Hyporheic Flow and Stream Ecology

Although this study does not examine the stream ecology associated with the thermal patterns of the stream, morphology of the stream or influences of the hyporheic zone they are all justifications for this study. Here is a short examination of literature pertaining to hyporheic flow in small streams and the influence on ecology. A good overview of the influence of subsurface-surface water exchange on stream ecology, specifically nutrient spiraling is by Mulholland and DeAngelis (2000). High ratios of surface area on sediment in the substrate to water volume and the nature and slow rate of advective flow through a saturated media retard the movement of nutrients downstream are two points examined in this work (2000). Pringle and Triska (2000) examine the influence of hyporheic flow on biological patterns in a stream. Other studies have

examined the importance of hyporheic flow in oxygenating salmonid eggs in redds (REF). Some of the biological effects are a result of distinct patterns of temperature, pH, redox potential, dissolved oxygen and nitrate associated with hyporheic flow (Franken et al., 2001).

1.4.3 Stream temperature and the Heat Budget

A historical summary of river and stream temperature research is provided in the introduction of Vugts (1974), but these studies do not necessarily make the connection between stream temperature and meteorological parameters. One of the works summarized is by Guppy who analyzed stream temperatures for the Nile from 1892-1897 concluding that: shallow streams are well mixed and have similar temperatures at the top and bottom, lowest stream temperatures occur just after sunrise, and maximum summer temperatures occur between the 15 and 16 hour (1974). Vugts comments that the first quantitative research of meteorological and stream temperature is by Eckel and Reuter (1950), their paper uses meteorological and stream temperature data to check theoretical formulae. Although interesting these studies do not directly pertain to the heat budget approach used in this study.

This study is built upon previous attempts at using a heat or energy budget model to predict stream temperature changes. Here we examine studies the prelude and influence this work. Many studies have used the heat budget in varying detail to model stream temperature; a good place to start with is the study by Brown (1969). Brown was the first to use a heat energy budget with measured meteorological data to predict stream temperature for an interest in water quality and using stream temperature as an environmental index in a small headwater stream. Small streams in western Oregon were

used for Brown's 1969 study with the purpose of illustrating the energy budget approach to predicting stream temperature as a management tool. Prior to the advancement in meteorological equipment the detail of this study was not possible. The addition of calculated bed-conduction values for the energy budget improved the understanding of the process of stream temperature change. Bed conduction is calculated by measuring a temperature gradient in the bed at unspecified depths. The model used included five flux terms: net thermal radiation, evaporative, conductive, and advective. Advective terms were assumed negligible, with only three terms (net radiation, evaporation and bed conduction) remaining in the budget equation. Radiation and evaporation were determined to be the dominant budget fluxes leading to temperature change. Brown states that the added bed-conduction flux is essential to model accuracy, the values for bed-conduction were small possible due to the neglected subsurface hydrology terms (hyporheic and groundwater flow). With variability in stream cover Brown encountered difficulty with direct sunlight on the radiometer. Because net radiation is the most important flux, shading was an important landscape variable, but was not quantified. In a later model (1970) Brown simplified the energy budget to include only net-radiation as an empirical relationship with stream temperature; due to the dominance that net-radiation has on small streams.

Vugts (1974) used a heat budget approach to measure meteorological effects on stream temperature, night time temperatures compared well with energy budget model predicted values, but a greater error was associated with day time temperature predictions. Vugts relates the discrepancy of daytime stream temperature predictions as a result of neglecting a groundwater component in his energy budget model. Net radiation

was measured approximately 30cm above the stream by a radiometer, corrected for by estimated percentage shading.

Comer et al. (1975) used interdisciplinary integration of water and soil mechanics for heat transfer. The model used was a one-dimensional conservation of mass equation, a partial differential equation that includes transport, advection and dispersion. The model was broken into three parts, a water column, interface and bed soil column; transfer of heat between the columns through advection and dispersion resulted in the heat budget, resulting in a prediction of streambed or interface column temperature change. They used an exponential attenuation equation for the amount of solar radiation absorbed into the streambed (Dake and Harleman, 1969) that is also used in this study. The conceptual model included groundwater into the soil providing heat, and between the soil water interface, this may be viewed as an early recognition of a hyporheic component in an energy budget.

Webb and Zhang (1997) conducted a stream temperature study in eleven reach locations in the Exe Basin, Devon, United Kingdom over a 21-month period allowing for comparison of heat budget components between different seasons of the year. The model incorporates conservation of heat and conservation of mass as a heat advection-dispersion equation. Improvements on previous studies by Webb and Zhang include advances in equipment used, they also installed the equipment at the stream site for local hydrologic and meteorological variable measurements. By measuring at the stream site effects of the local stream environment on the microclimate of the watercourse are incorporated.

Fluxes included in the heat budget are net radiation, evaporation/condensation, bed conduction, sensible heat exchange, fluid friction and advective heat fluxes. The

advective heat fluxes include heat transfers in precipitation and groundwater calculated from measurements of the volume and temperature of the flows involved. To capture groundwater they used stage measurements at upstream and downstream boundaries to account for change in flow, by correcting for evaporation they estimated the rate of groundwater exchange. This method is very subject to inaccuracies, so I used this method only to show that the groundwater component was operationally negligible and that the hyporheic exchange component captured the important groundwater component during low flow summer months. Webb and Zhang (1997) found that net radiation was the dominant energy budget component but the measured net radiation values could be reduced by one-fifth of the value measured at a height of 30cm due to bank shading.

In a similar study Webb and Zhang (1999) investigated the influence on diel and diurnal variation of stream temperature on two watercourses. The streams dominated by groundwater flow have a subdued water temperature variability reducing the sensitivity of the air and water temperature relationships. Non-advective energy gains were again dominated by net radiation, followed by condensation, sensible heat transfer, bed conduction and friction. Exposed channels received more net radiation, also evaporation fluxes increased as well. This study also points out the need for longer-term heat budgets; most existing are less than five days.

There are many additional studies that examine stream temperature, (Isaak and Hubert 2001; Melina et al. 2002) these studies often focus on a specific parameter (aspect, stream width, watershed size, canopy cover) and the potential effects on stream temperature. A study by Mohseni and Stefan (1999) compared stream and air

temperature patterns and showed a strong correlation for physical interpretation, a similar relationship is established in this study.

Constantz (1998) shows that small stream temperatures have a greater diurnal variation when they are losing flow to groundwater, and that in gaining stream groundwater acts as a buffer. Despite many attempts at modeling longitudinal change in stream temperature using a heat budget few studies have incorporated subsurface and surface water interaction other than gains or losses of groundwater, Moore and Sutherland (2002) and Story et al. (2003) imply the importance of hyporheic exchange influence on stream temperature. Story et al. (2003) estimated that hyporheic exchange was an important contributor to downstream cooling in a headwater stream associated with alternating forest and clear-cut. Hyporheic flow was a significant factor in cooling stream temperature longitudinally when there was little gain in flow from groundwater. Storey et al. also link the degree of bed conduction to the degree of groundwater influence in the streambed.

Moore et al. (2004, in press) observed spatial heterogeneity in bed and stream temperatures at various spatial scales in a mountain stream in British Columbia. Moore et al. show that bed temperatures during summer months were lower in upwelling zones related to surface-subsurface interactions and the influence of hyporheic exchange. The spatial and temporal temperature patterns in the stream varied greatly. Down welling zones tended to have greater diurnal variation in stream temperature and higher mean temperatures. Moore et al. (2004, in press) calculated hyporheic flow using Darcy's law by measuring the vertical hydraulic gradient between the stream and substrate, the calculated flow was converted to a heat flux and included in the heat and water budget for

the stream. Net radiation was the dominant flux and sensible and conductive heat exchanges were minor during the day. Latent heat and groundwater inflow were also minor terms in the budget, both tended to cool the stream during day and the night. Hyporheic flow was found to have a warming trend on the stream during the night and cooling effect during the day. Sensible heat loss associated with evaporation and heat generated by friction were negligible in this study.

1.4.4 Hyporheic Flow

Recently research has focused on the interaction of subsurface and surface flow due to the recognition of the importance of the flow paths by ecologist and hydrogeologists. Hyporheic flow is the advection of stream water through and interacting with underlying sediment, bedrock and groundwater and returning to the stream. Hyporheic flow is driven by hydraulic gradient between the stream and the head in the substrate controlled by morphology and substrate properties. Multiple scale flow paths of hyporheic flow occur in streams. These flow paths repeatedly bring stream water into close contact with geochemically and microbially active sediment (Harvey and Wagner, 2000; Findlay, 1995). Kasahara and Wonzell (2003) showed that step-pool sequences caused exchange flows with relatively short residence times. In step pool streams flow is forced into the subsurface through a riffle and emerges in the pool below the step.

Two main approaches have been applied to estimating hyporheic flow in small streams, a Darcy groundwater approach using hydrologic head data in the stream and subsurface, and an indirect method by measuring the breakthrough curves of an injected

tracer behavior in a stream (Harvey and Wagner, 2000). A third approach of calculating hyporheic flow uses measured vertical temperature profiles through the substrate and viewing temperature as a tracer. This method is used as a check on the tracer method results. A simplified approach modified from Constantz et al. (2003, 2002) is used in this study.

Due to potential for stream disturbance and difficulty in installing piezometers through cobble substrate the Darcy groundwater approach was also used only for a check against results from the tracer method in this study. To estimate the flux rate of stream water through the hyporheic zone we used a one-dimensional model of advection and dispersion that includes a term for coupling the active channel with a slow moving zone or transient storage zone (Bencala and Walters, 1983; Harvey et al., 1996). Using the tracer method assumes that the hyporheic zone leaves an imprint on the tracer behavior.

2. SITE DESCRIPTION

2.1 Geographic Location

This study takes place in a semi-arid environment in a small headwater stream along the Boise Front in the Dry Creek Experimental Watershed. Dry Creek is located in southwestern Idaho approximately 7km north of Boise. (Figure 2.1). The experimental watershed has its headwaters in public U.S. Forest Service land at approximately 2100-meters elevation and terminates where the stream passes under Bogus Basin Rd at approximately 1000-meters elevation. The primary research focus in this watershed is cold-season stream flow generation; hill slope hydrologic transfer processes, hydrograph separation methods and mountain front groundwater recharge rates. A short 400-meter

reach is considered for modeling stream temperature change longitudinally by measuring and calculating major heat energy fluxes interacting with the stream. The study reach is accessed by single track trails that follow the Dry Creek valley. Downstream of the 400-meter study reach, near mid-basin, Dry Creek confluences with Shingle Creek nearly doubling the drainage area and stream flow. Dry Creek continues west-southwest to confluence with the Boise River. Although Dry Creek and Shingle Creek are perennial within the experimental watershed Dry Creek dries during summer months before it passes underneath State Highway 55, approximately 12-kilometers downstream of the mouth of the experimental watershed.

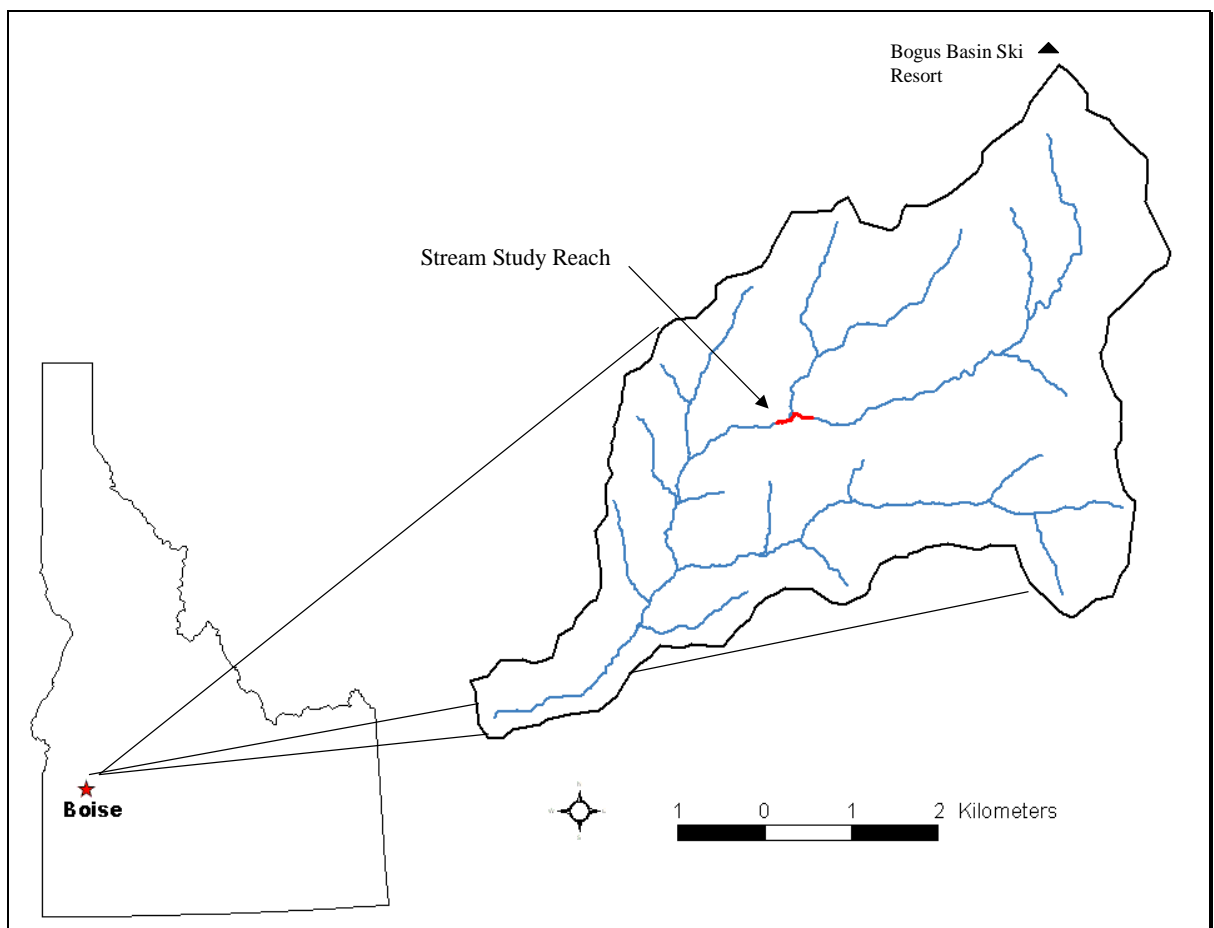


Figure 2.1. Dry Creek Experimental Watershed Stream Study Reach and regional location maps.

Currently land within the Dry Creek Watershed is used for rangeland for cattle and sheep and recreation, with some timber harvest. Forty-two percent of the land is U.S. Forest Service (11.52km^2 , 2846 acres), the Bureau of Land Management owns 0.05 km^2 (11.06 acres) the State of Idaho 0.70km^2 (162.09 acres) and the rest is privately owned (15.10km^2 , 3729.42 acres). The study reach lies entirely in private land and is accessed by a public use trail that follows Dry Creek from Ridge Road to Bogus Basin Road.

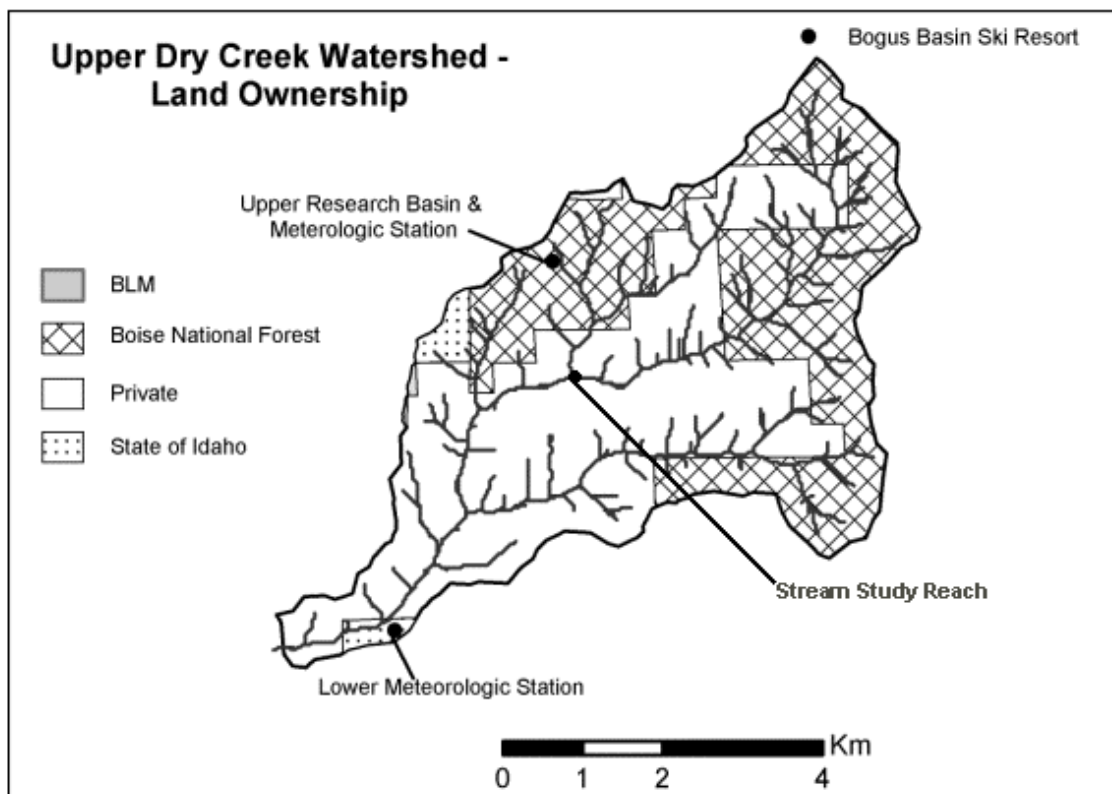


Figure 2.2 Landownership within Dry Creek Experimental Watershed (modified from Yenke, 2004).

2.1.1 Climate

The basin has a moderate climate with frozen soil in the lower regions, below 5000 feet elevation. In the transitional zone there is a intermittent snow pack during winter months. The upper elevations have a consistent snow pack through out the winter, spring melt transfers to the stream network resulting in peak annual flows. Flows steadily decrease during the hot, dry summer months. Summer months receive very little precipitation from occasional convective thunderstorms.

2.1.2 Geology

Dry Creek Experimental Watershed is located in the Boise Front Mountains north of Boise. The front is the northern boundary of the western Snake River plain on the northern boundary of a half-graben formed basin where Boise and Ada County reside. The Cretaceous Idaho Batholith, a granite-granodiorite intrusive body that is heavily fractured and makes up the hills of the Boise Front, underlies the Dry Creek Experimental Watershed. The Idaho Batholith is made up of two lobes, Bitterroot and Atlanta lobe, the Dry Creek Watershed lies within the southern Atlanta lobe. At lower elevations in the geology of the watershed is composed Tertiary Lake Idaho sediments of the Terteling Springs xx group (Wood, unpublished Boise North Quadrangle). The Terteling Springs xx formation consists of lacustrine and transitional sedimentary facies including unlithified or lightly lithified sands and conglomerates, oolitic beds and fine-grained silt or clay beds.

2.2 Physical Characteristics

The basin is 27 square kilometers in area and is drained by a small 2nd order stream. The watershed is accessed by Bogus Basin Road, which leads to a local ski resort of the same name.

2.2.1 Stream Flow

Wintertime snow accumulation and the timing of snowmelt control stream flow in the region. Through out the year the transfer of water down slope as unsaturated flow through soils and saturated flow as groundwater control the timing of stream flow in ephemeral and intermittent streams, and is one of the primary research foci in the Dry Creek Experimental Watershed (ref thesis and papers). Stream flow is measured at 7 locations in the basin, 5 of the locations are ephemeral and show a pattern of flow peaks coinciding with spring snow melt (map showing gauging stations). High flows in the spring quickly recede during summer months. Intermittent streams cease to flow during summer months and do not start to flow again until a persistent snow pack exists at the upper basin.

Stage is measured at each of the stations by a caged pressure transducer; flow is related to stage by repeated measurements and the development of a rating curve. The flow at the study reach, Confluence-1-East (C1E), was used to control steady flow; although flow fluctuated diurnally during the study period there were no large changes in flow during the study period (figure showing pattern of flow at con 1).

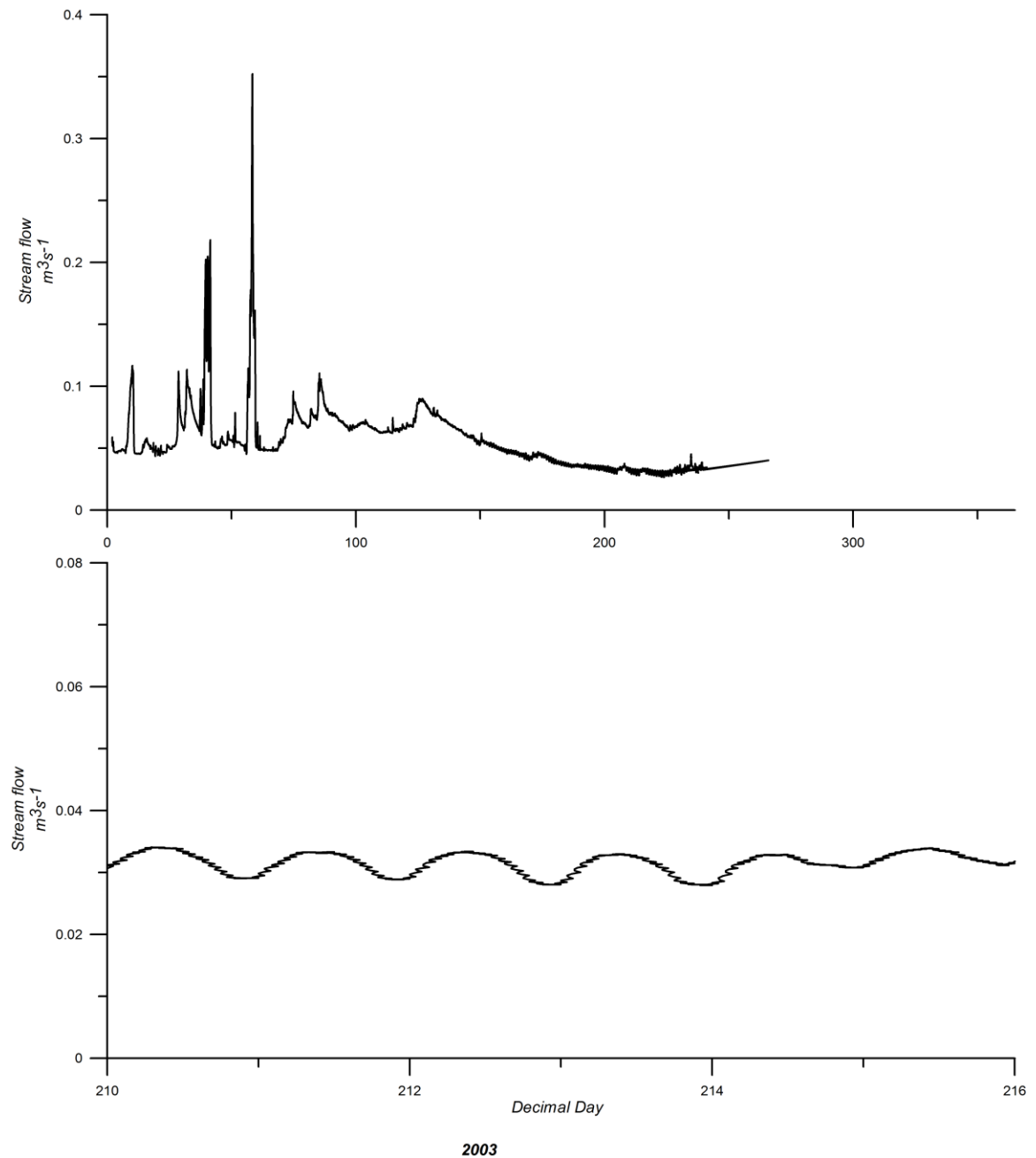


Figure 2.2.1.1. Top, an incomplete annual hydrograph measured near the top of the study reach. Bottom hydrograph shows the daily stream flow pattern during the study period.

Gauge locations at a lower confluence and at the mouth of the watershed at Bogus Basin Road are used to show longitudinal flow patterns and to make inferences about stream-groundwater interactions. Regrettably, the gauge at Confluence-2-West (~2.5km

downstream of C1E) was unstable, the pressure transducer itself and its location as well as persistent battery problems make any data collected at C2W unreliable. The lowest gauge in the watershed, Low-Gauge, was established ~5 years ago and was well calibrated to flow. Days before the beginning of the field campaign, data from Low-Gauge stops, after brief investigation the reason was determined to be theft; before 1pm on the July 28, 2004 (Dday 209) the data logger was disconnected from the pressure-transducer and removed with the solar panel. Theft was not considered prior to this study.

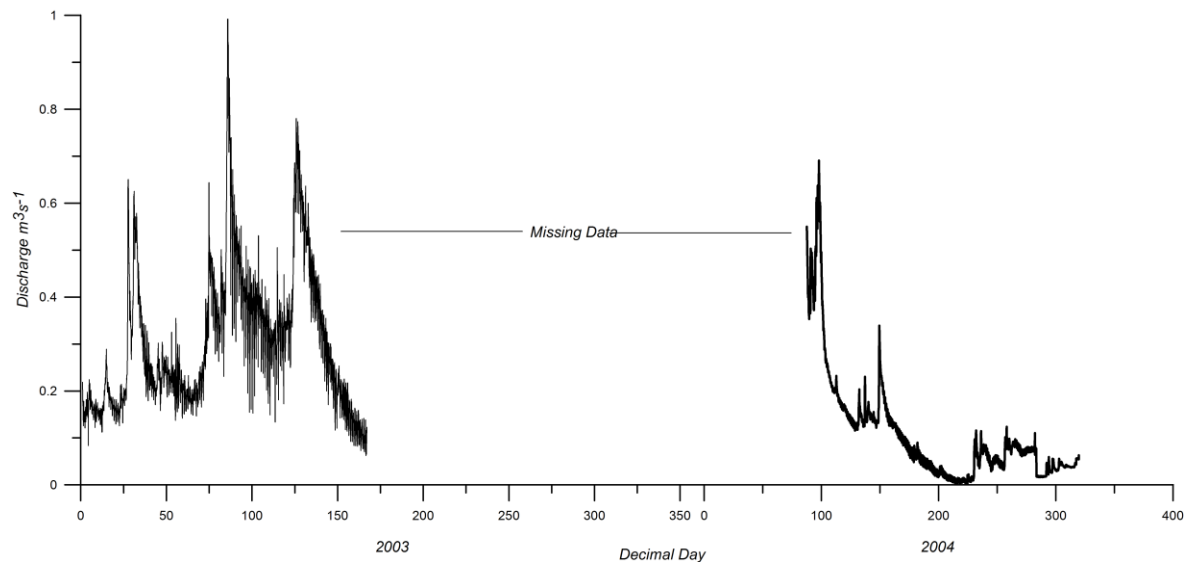


Figure 2.2.1.2 Low gauge hydrograph for 2003 and 2004. Missing data is due to theft of pressure transducer.

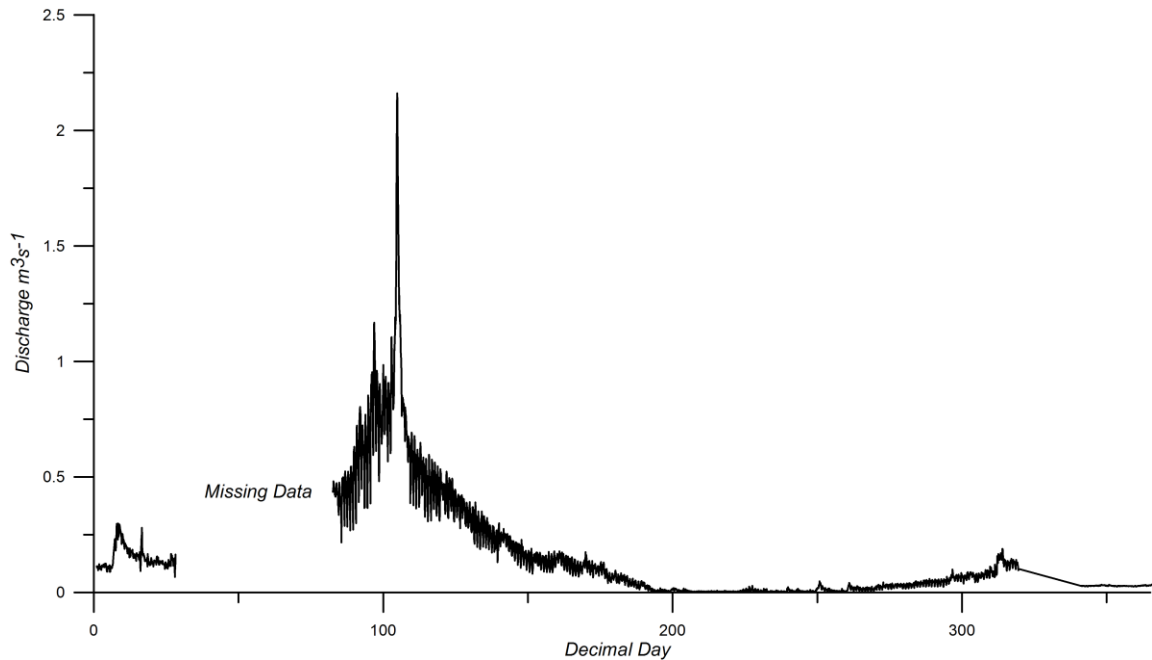


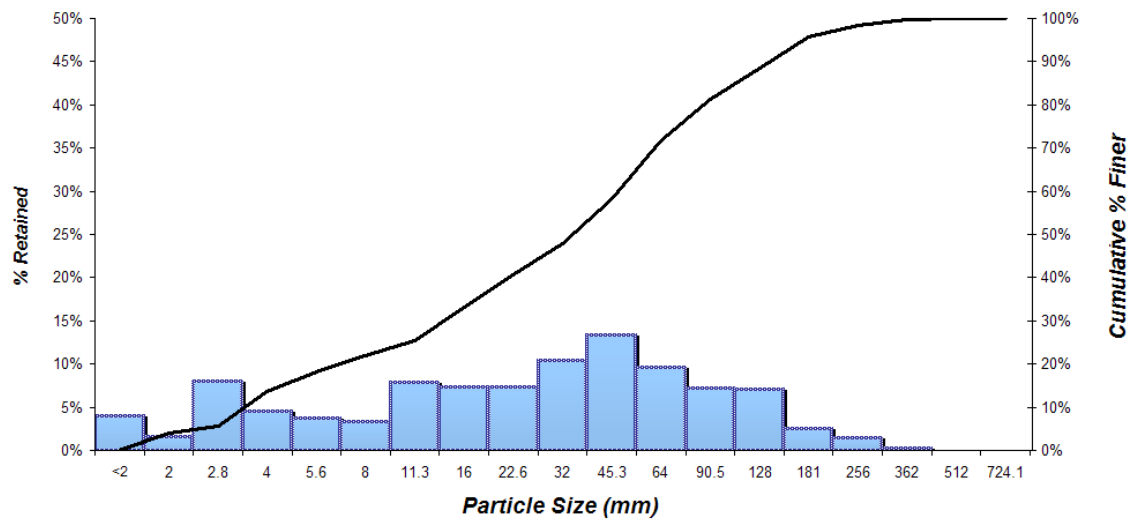
Figure 2.2.1.3. Low gauge hydrograph from 2002. Peak in the spring during snowmelt.

2.2.2 Reach Morphology

Through out the experimental watershed the local geology controls stream gradient, valley confinement and substrate, as bedrock or large colluvial inputs. As Dry Creek flows out of the hills of the Idaho Batholith and into the Boise River valley the gradient and confinement decrease changing the morphology to a pool riffle stream. The lower section of Dry Creek steadily loses flow to groundwater and evaporation, and soon disappears as the name Dry Creek implies.

In the upper-basin, including the Experimental Watershed the stream morphology tends to be step-pool or proto-step-pool where the pool tail-outs resemble riffles and steps are less defined. The study reach was chosen for its high gradient, perennial flow and hydraulic effects caused by the reach morphology. Within the study reach pool spacing is an average of 7-meters; each pool has a long tail-out or riffle before the next step into a

pool. The morphology specifically within the study reach is a low-gradient step-pool where pools are scoured by pour-over below cobble, boulder, bedrock steps and sometimes by scour associated with woody debris. Each pool has a long pool tail outs that resemble riffles. The substrate was analyzed by a surface pebble count (Wolman, 1954); the count was modified to capture morphology specific trends, counts were conducted discretely in pools and riffles to classify each morphology. The substrate is dominated by coarse gravel and cobble (Figure grain size) with occasional bedrock outcrops; the coarser sediment is input by hill slope processes and is not transportable by stream processes. Pool and riffle surface grain size distribution are very similar but pools have a distinct sand component. Presumable the pools retain surface fines during summer low flows giving the appearance of an overall finer substrate.



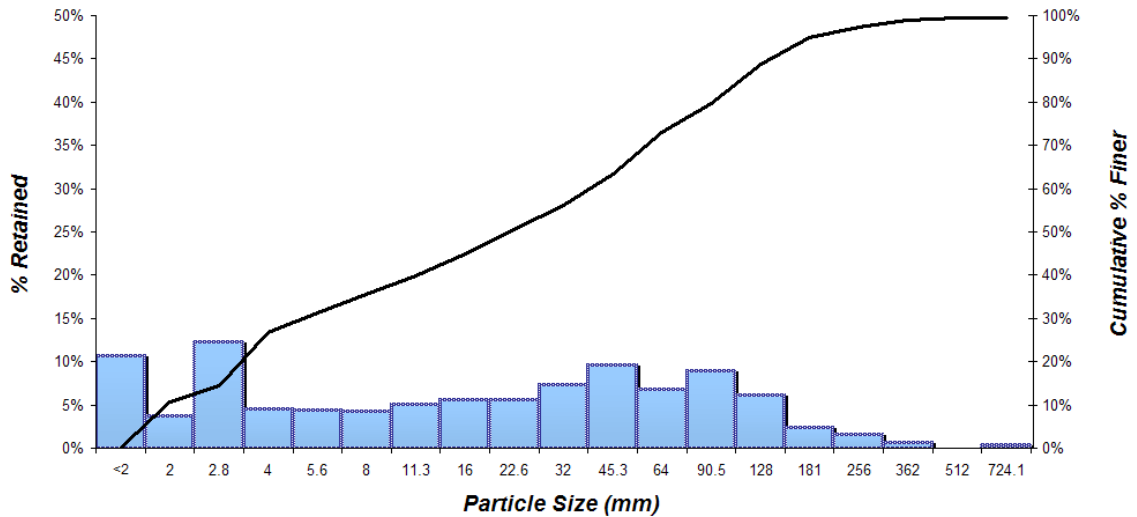


Figure 2.2.2.1. Top shows average grain-size distribution for riffles. Bottom shows grain-size distribution for pools. Both graphs have a cumulative-percent-finer graph and grain-size distribution as a histogram.

2.2.3 Vegetation

The study watershed transitions from montane at the upper elevation (~7000 ft) to desert steppe, at lower elevation (~3000 ft) of the catchment, the channel is heavily shaded by riparian vegetation. The study reach is mid-basin with vegetation dominated by water birch (*Betula occidentalis*), service berry (*Amelanchier alnifolia*) various willow (*Salix spp.*), Rocky Mountain Maple (*Acer glabrum*), wood rose (*Rosa woodsii*), Douglas Fir (*Pseudotsuga menziesii*), and some Ponderosa Pine (*Pinus ponderosa*). The hill slopes away from the active channel have significantly less shade, dominated by sage brush (*Artemisia tridentate*), cheat grass (*Bromus tectorum*) with occasional ponderosa pine (*Pinus ponderosa*).

This stream supports an isolated group of red-band trout, and the stream morphology is typical of many mountain front streams in the inter-mountain west that

may be habitat, spawning and rearing grounds for endangered bull-trout and other salmonids.

3. Temperature Measurements

3.1 Introduction

This study examines the thermal regime of a headwater stream in a semiarid watershed. Temperature measurements are necessary longitudinally in the channel as well as in the substrate to fulfill the goals of this study. The measured in-stream temperature and change in temperature longitudinally are used to calibrate and analyze the heat budget model predictions of temperature change.

This study focuses on the change in temperature through the reach rather than predicting the absolute temperature. By examining the change in temperature the upstream boundary temperature is not needed; this method also allows us to examine smaller temperature changes.

Prior to the summer of 2003 the study stream reach in Dry Creek was instrumented with vertical thermistors through the substrate in two separate riffle-step-pool sections. The thermistor columns were inserted in adjacent pool and riffle pairs, one near the upstream boundary of the study reach and one near the downstream boundary of the study reach. A total of 5 different columns were installed, 3 in the upper pool-riffle pair and two in the downstream pair. The thermistors were driven through the substrate to measure temperature at depths below the stream. The thermistors measured temperature at the stream/substrate interface, at 5cm depth, at a depth between 15-20cm and at a depth range of 30-35cm depths, depending on the difficulty in insertion.

Temperature change for the first 40-meters of the study reach were made using thermocouple wire, recorded at the insulated Campbell Scientific CR10X data logger. The thermocouple wires in the stream were fastened inside of plastic pipe several centimeters above the stream bottom. The thermocouple measurements did not reference a thermistor temperature.

Absolute temperature is measured at 8 places by Onset Tidbits along the reach to characterize the temperature patterns of the reach, for the 400-meter reach length Tidbits were also used to measure the longitudinal temperature change.

Results in this section as well as other sections dealing with time variable parameters will be presented for the entire study period as well as summarized as a 24-hour average, where the study period is reduced as averaged into a typical 24-hour period. The daily average temperatures patterns are reported for the study period to allow for simple comparison of the measured and modeled temperature data and to allow for detailed examination of the typical thermal regime patterns for a summer day.

3.2 Methods

Stream temperature was measured by three different methods. Absolute temperature and temperature change for the 400-meter reach distance were measured by Onset Tidbits, temperature change for distances 10 and 40-meters are made by thermocouples. Thermistor columns measure vertical temperature profiles through the substrate. The following text explains in more detail the temperature measurements.

Downstream longitudinal temperature change was measured using thermocouple wire in a PVC shelter to prevent sun light from hitting wire directly. The temperature measurement was made five to ten centimeters above the substrate. Thermocouples can measure absolute temperatures in environmental ranges accurate within $\pm 0.2^{\circ}\text{C}$ with a reference temperature provided with a thermistor. By removing the reference temperature and controlling the temperature of the thermocouples at the data logger we can measure relative temperature of each thermocouple station with more precision but sacrifice absolute temperature measurements. Absolute stream temperature at 8 locations was measured using Tidbit submersible temperature loggers accurate within $\pm 0.2^{\circ}\text{C}$. The results from four temperature measurement locations by the tidbits are shown because many of the sensors were placed in close proximity or in the same morphologic unit and did not show a difference in temperature. The four locations shown are at the upstream boundary (0-meters, reach distance), 20-meter reach length and 400-meter reach length.

Many of the homemade thermistors went bad or deviated from the tidbits for in-stream temperatures. Thus the thermistors are not the better absolute temperature measurement, but are useful to show vertical temperature patterns through the substrate. Multiple vertical thermistor columns were used to estimate hyporheic flux rates, where only timing of temperature change is necessary (Section 4.2.3). The column located in the riffle at the upstream boundary was used for the vertical temperature gradient through the substrate.

The thermocouple wire used in the field was tested in the laboratory for accuracy. The test consisted of the same wiring design used in the field; the measurement ends of the thermocouple are placed in an isothermal water bath used to check the temperatures against each other. All thermocouples were placed within a 5cm radius to assure the same ambient temperature at each sensor. Ideally all sensors should read the same temperature and the error is determined by observing the average difference between each of the sensors. The temperature deviation measurements change averaged an error of 0.005°C over a 6-day test period.

3.3 Results

3.3.1 Longitudinal Temperature Pattern and Temperature Change

Daily maximum temperatures would increase at all locations until reaching a peak in the early evening between 7 and 9pm before the temperatures would start decreasing. This trend follows the daily air temperature patterns (Figure 3.3.1). The sensitivity of stream temperature to air temperature was examined by calculating the covariance coefficient for four stream locations against air temperature at the weather station for the average 24-hour period. The sensitivity of stream temperature increased downstream. The stream temperature at the upstream boundary had a relatively low correlation coefficient ($r_{\text{stream-air}} = 0.23$) compared to values at 15m ($r_{\text{stream-air}} = 0.66$), 40-meters ($r_{\text{stream-air}} = 0.51$) and 400-meter ($r_{\text{stream-air}} = 0.53$) measurement location.

With increased distance of stream length the range of temperature variation and maximum values increases. The highest daily temperatures occur at the down stream boundary, 400-meter reach distance usually peaking late in the day around 7 to 9pm.

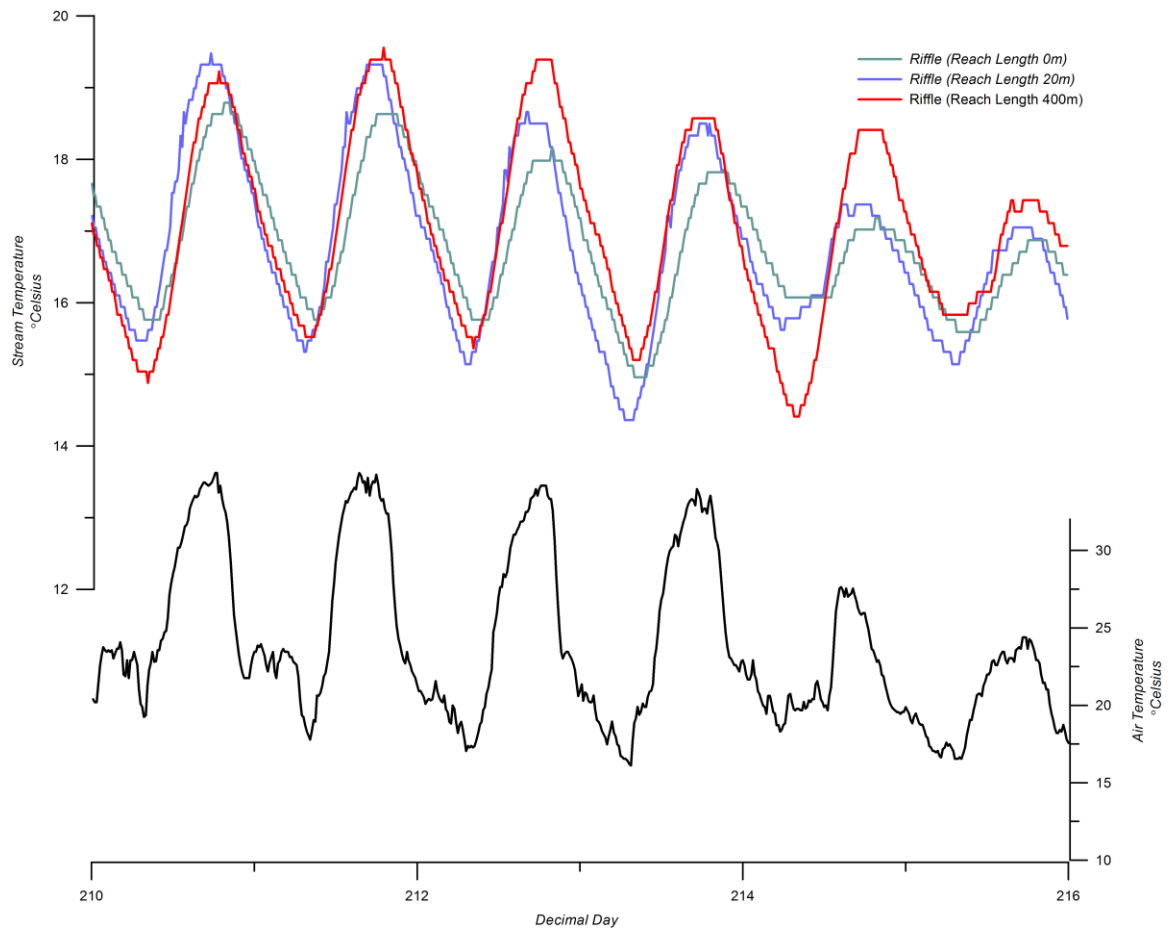


Figure 3.3.1.2. Daily trends of air temperature and longitudinal temperature profile measured in riffles.

On average the downstream boundary sensor (400-meter reach length) would peak at approximately 18.5°C daily, the upstream boundary would peak at half a degree lower, just under 18°C (Figure 3.3.1.2).

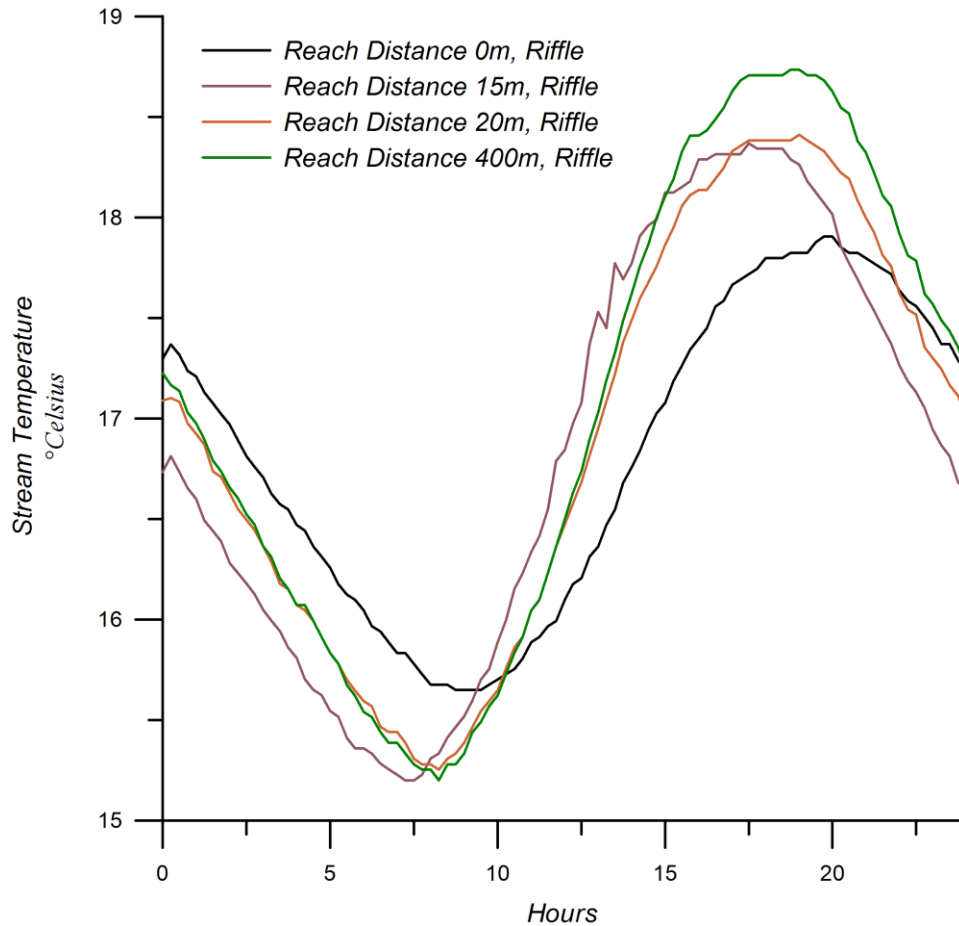


Figure 3.3.1.2. Daily averaged longitudinal temperature patterns for the study period, Julian Day 210 to 216.

In general stream temperature increases downstream, figure 3.3.1.1 and 3.3.1.2 both record temperature in similar morphologic features, down-welling riffles. Figure 3.3.1.3 views temperature in a down-welling riffle at the upstream boundary and an adjacent up-welling pool. Pools are features associated with returning hyporheic flow show no increase in temperature from the adjacent upstream riffle (Figure 3.3.1.3). By examining the same location as a daily average for the study period the difference between the temperature measurement locations are more defined, the slight decrease between the upstream riffle and the downstream pool is more evident and the tail of the

pool is also included showing a sharp increase in temperature downstream (Figure 3.3.1.4). This shows the heterogeneity of the longitudinal stream temperature on a morphologic feature scale.

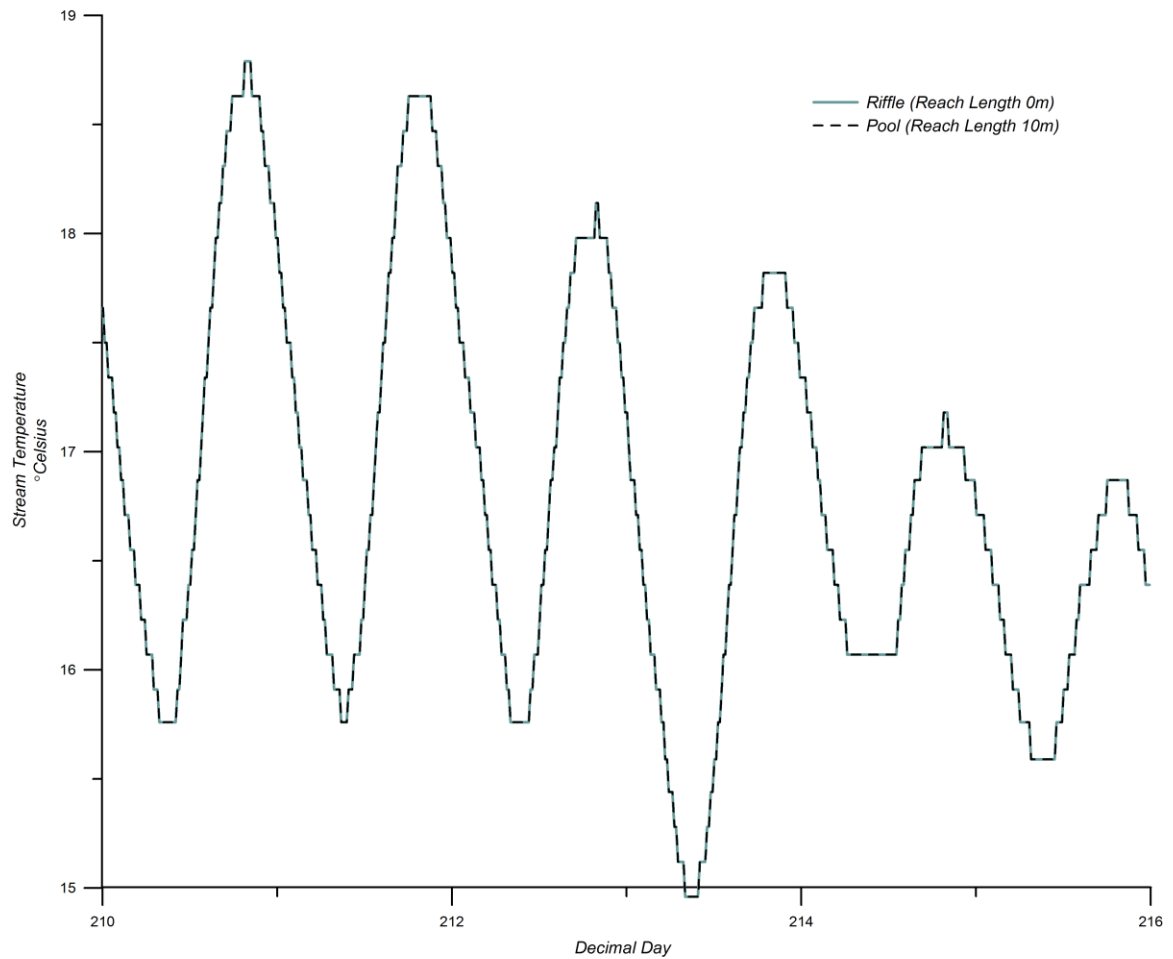


Figure 3.3.1.3. Longitudinal temperature pattern between adjacent pool and riffle during study period.

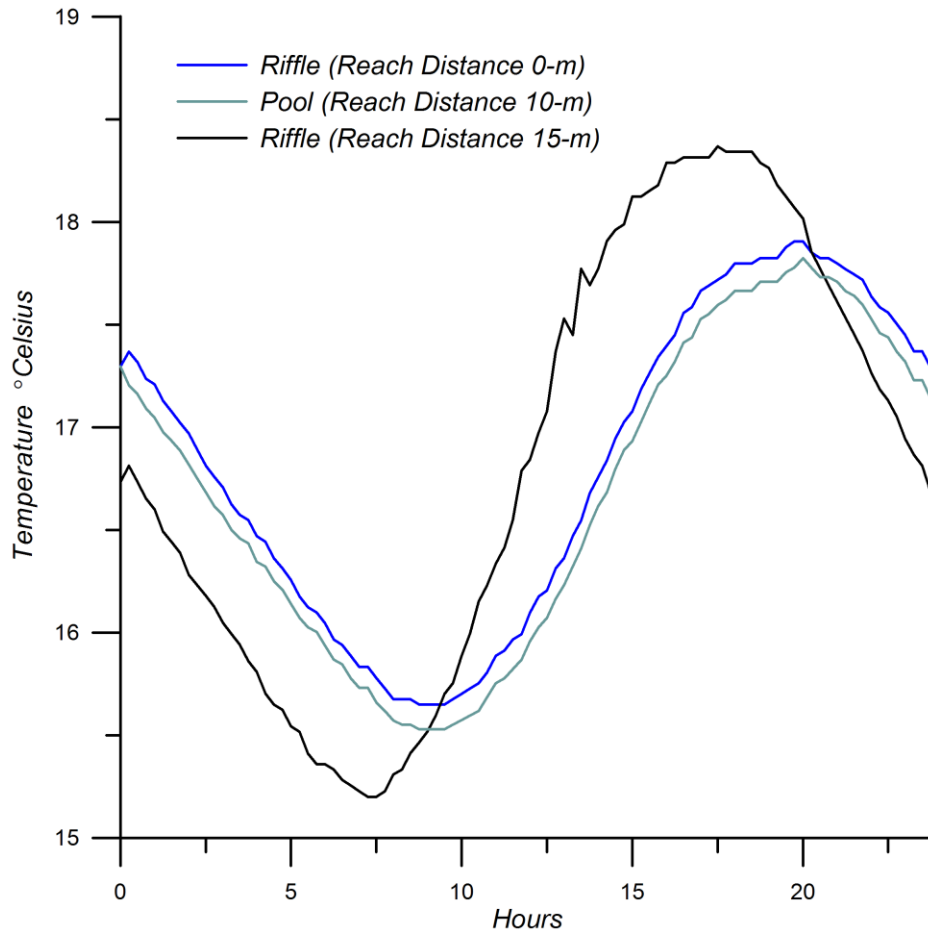


Figure 3.3.1.4. Daily averaged longitudinal temperature patterns between the upstream boundary riffle (0-meters) an adjacent up-welling pool (10-meters) and the tail of the pool another down-welling riffle feature (15-meters).

Examining temperature change in more detail by the thermocouple measurements show a general trend of warming downstream during the daytime, coinciding with solar radiation and high air temperatures. By examining the daily temperature change, averaged over the study period, a typical trend in heating and cooling for each reach length can be analyzed. Figure 3.3.2 shows the measured temperature change from the top of the study reach downstream 40-meters, the change is determined by simple subtraction of the two measurement locations. The temperature slowly stops decreasing

by 8am starts to increase around 10am through the early day, but the measurements have an odd dip in temperature change during the early afternoon. This is possible an affect of local energy fluxes that cause a mid-day cooling for this reach length, where the energy fluxes out of the stream dominate most of the day, but more likely this is an inaccuracy due to measurement location and equipment. The temperature does start to descend from peak rates of temperatures increase around 9pm reaching a maximum magnitude decrease just before at around 8am.

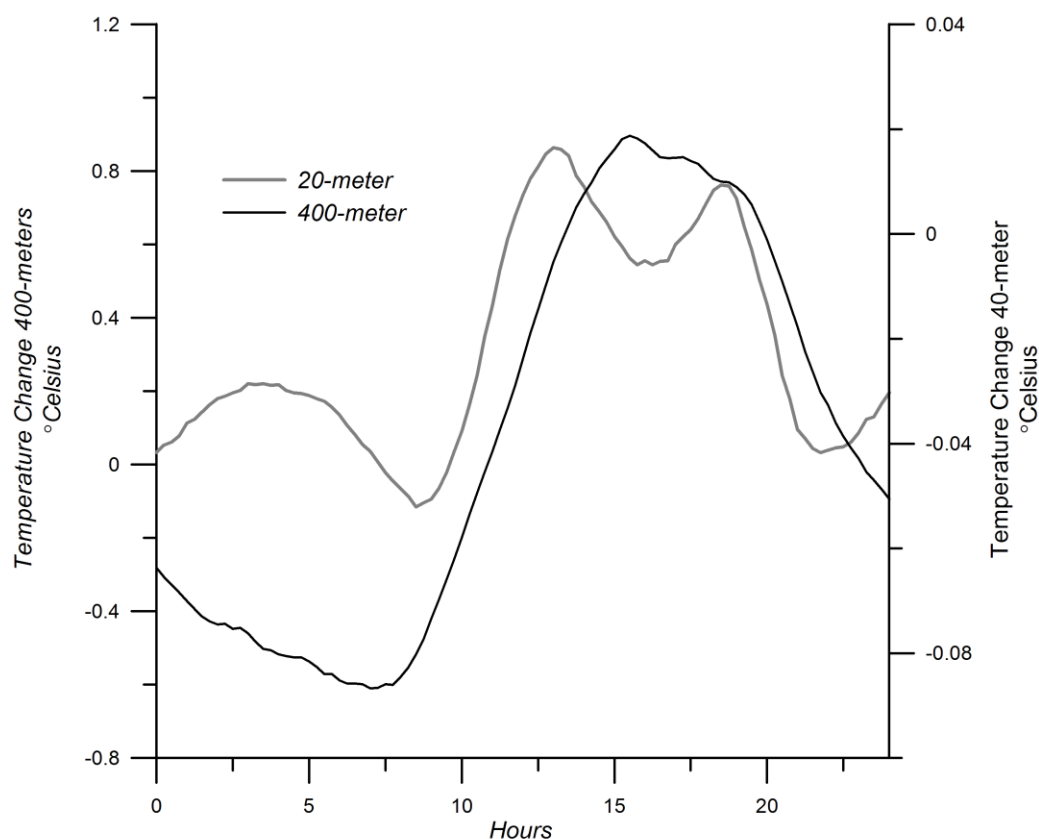


Figure 3.3.1.5. Temperature change measurements for the 40 and 400-meter reach lengths.

The temperature change over the entire reach length, 400-meters, has a larger magnitude of change than the 20-meter reach distance. At its maximum increase just after 5pm the difference between the top of the reach and the bottom of the reach on average is around 0.8°C . After this peak in temperature change the rate decreases until it starts cooling at approximately 9:30pm. Temperatures continue to decrease over night and into the morning, after 10am the temperature start to increase between over the reach length.

3.3.2 Temperature Patterns in the Substrate

After calibration in the laboratory the thermistors deviated from each other greatly in the field. Although the absolute temperature measurements are unreliable the temperature patterns and magnitude changes in temperature are relative consistent between measurement locations. The upper riffle shows

These results are used in estimating hyporheic flow (section 3.something) as well as for calculating bed conduction.

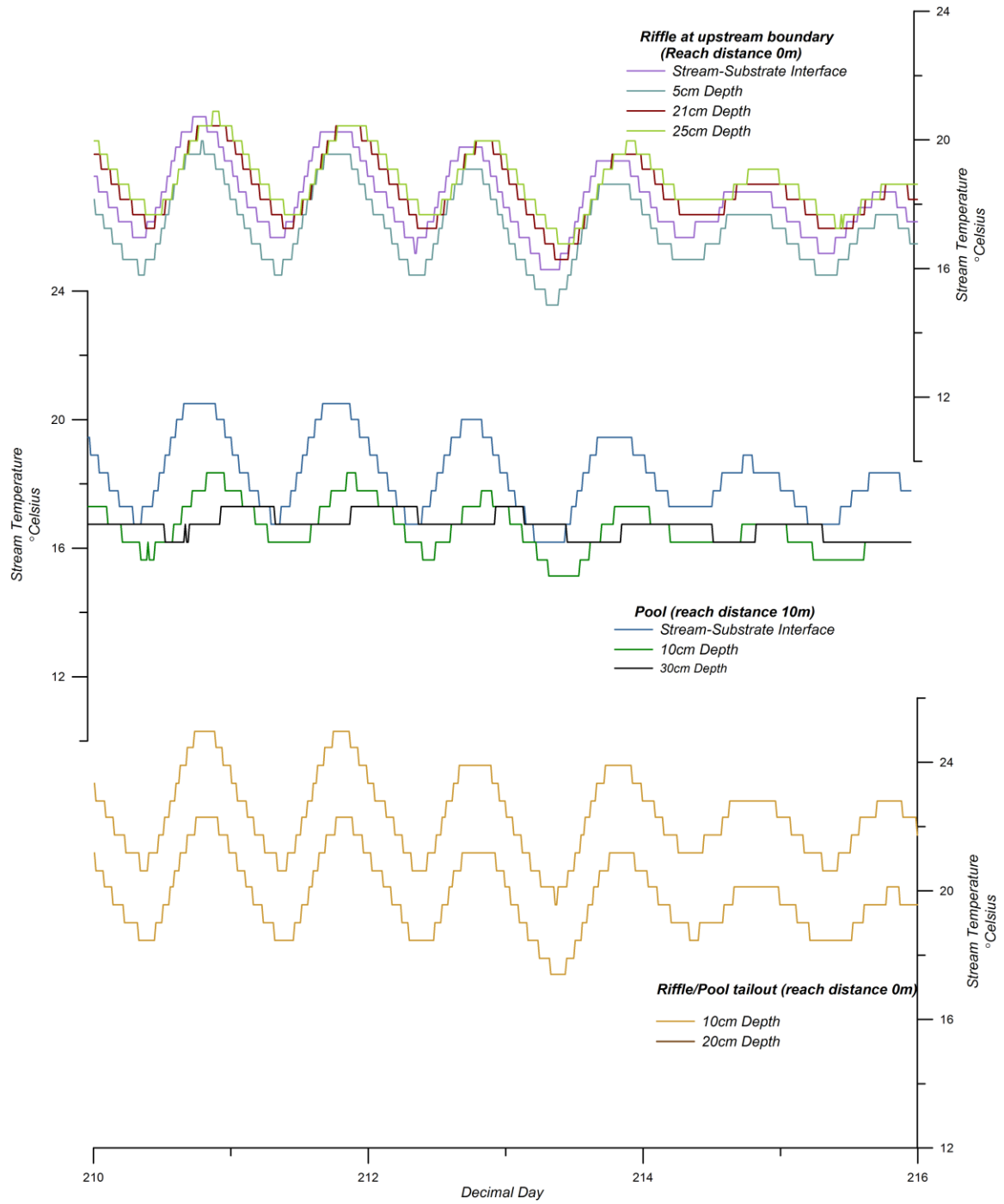


Figure 3.3.2. Vertical temperature profiles during the study period, these profiles are used in determined the bed conduction and hyporheic energy components.

3.4 Discussion

Generally temperature increased downstream during summer days, but we see heterogeneity in that increase. Viewing downstream temperature patterns measured in similar morphologic features the riffles shows warming downstream (Figure 3.3.1.1 and 3.3.1.2). No increase and possible slight decreases in longitudinal temperature occur over short stream lengths associated with pools; the processes involved in the pool specifically hyporheic flow returning to the stream at a lower temperature than the stream accounts for the longitudinal stabilization of stream temperature. This can be seen by figures 3.3.1.3 and 3.3.1.4, where the rising limb of the temperature profile does not increase as much in the pool features as in the temperatures measured in riffles. It is hard to imagine much temperature change over such a short stream length. Due to the change in hydraulics in the substrate and the returning flow, the pools are a buffer location for the overall down stream temperature increase. In the pool the cooler water returning from the hyporheic zone cools the stream flow and decreases the overall heating of the stream. Moore et al. (2005 in press) also observes the heterogeneity of stream temperature associated with morphologic features and related hyporheic flow.

The temperature profiles in the substrate show large daily fluctuations at depth associated with zones of down welling; the fluctuations have a much smaller magnitude in upwelling zones. For example in Figure 3.3.2 the riffles, down-welling zones, show very little temperature attenuation where as the pool, an up-welling zone shows dampened temperature fluctuations. Temperatures in the substrate below the pool have a smaller magnitude of temperature change daily; this is due to less influenced by the surface temperature changes. At shallower depths in the pool the thermistor located 10cm deep shows greater fluctuation presumable due to some mixing with surface water.

For changes in temperature at a 400-meter stream length tidbits were used with an increased measurement error. Due to the magnitude in temperature difference between the top and bottom of the study reach the error associated with the tidbit measurements is acceptable.

4. Hyporheic Flow

4.1 Introduction

In this study tracer experiments are used to determine hyporheic flow rates, two additional methods to measure and calculate hyporheic flow, independent of the tracer, are used to estimate and compare flow rate values. These additional methods are a hydrometric approach using Darcy's Law and an approach observing thermal patterns in the substrate at a down-welling riffle using temperature as a tracer. Heat as a tracer and the conservative chemical tracer experiment are similar in that they observe breakthrough curves to inversely calculate transient storage of the stream and hyporheic flow.

The hydrometric approach or Darcy approach uses Darcy's Law and direct measurements of hydraulic head in the substrate and in the stream. Regrettably the hydraulic measurements are insufficient in this study, not enough measurement locations were used to capture the flow for the entire reach. Due to potential for stream disturbance and difficulty in installing piezometers and vertical thermistor columns through cobble substrate the hydrometric approach and the temperature as a tracer method were used only for a check against results from the tracer method in this study.

The tracer method assumes that the processes involved in stream flow leave an imprint on the tracer behavior. After a chemical tracer is input into the stream the stream flow is observed at a fixed location over time, resulting in the measurement of the

breakthrough curve, the observation of the concentration of the tracer past this point over time is directly influenced by diffusion, possibly sorption, dilution by introduced water or lost water, and by the water flow paths.

To estimate the flux rate of stream water through the hyporheic zone we used a one-dimensional model of advection and dispersion that includes a term for coupling the active channel with a slow moving zone or transient storage zone (Bencala and Walters, 1983; Harvey et al., 1996). Using the tracer method assumes that the hyporheic zone leaves an imprint on the tracer behavior.

4.2 Methods

Hyporheic flow is a component of groundwater; it flows through saturated media controlled by hydraulic conductivity. Here it is assumed that all flow that infiltrates the substrate and return to the stream is hyporheic flow, flow that does not return to the stream or waters that return to the stream and exceed the loss are also groundwater. Groundwater loss or gain was measured by repeat stream flow measurements at the top and bottom of the reach.

4.2.1 Tracer Experiments

Multiple tracer experiments were conducted but only two were recorded and modeled successfully. The others were successful in that they provided useful procedural information, but regrettably each was uniquely unsuccessful in recording the necessary data for modeling. Two successful tracer experiments are presented here, the first was a slug injection during the heat budget component measurements in July 2003. The second was a constant rate injection early the following summer, June 2004.

A chloride tracer was used due to the conservative nature of chloride. The slug was introduced as a pulse by dissolving table salt in 20-30 liters of water and pouring the tracer into the stream upstream of the study reach. The sensors for the two slugs were xx specific conductivity sensors wired into a Campbell CR10X data logger, and a handheld conductivity sensor. The first sensor is located ~30-meters downstream of the injection point, to allow for complete mixing of the tracer with in the stream. The first sensor point is used as the upstream boundary condition and is referred to as the arbitrary starting point or distance 0-meters. The other sensors are measured relatively to the upstream boundary condition sensor. The downstream sensors were located ~60-meters and 400-meters downstream.

The constant rate injection used both chloride and rhodamine for conservative chemical tracers; two stations were installed, both equipped with a fluorometer and conductivity. A peristaltic pump was used for the steady injection, the input hose was placed in the bottom of a 5 gallon bucket with well mixed tracer solution and the output end was anchored in midstream near a small rock pour over to allow for quick mixing. The upstream sensor was a data sonde called a Hydrolab. A Campbell Scientific CR10X

logged the downstream boundary measurement location with a conductivity sensor and a Turner Designs Cyclops-7 fluorometer.

The constant rate injection experiment was only recorded at one location, the farthest downstream sensor, 400-meters. The data sonde did not record the experiment due to a user error. A boundary input was estimated at the injection site from the injection rate (Q_{Solution}), stream flow (Q_{Stream}), injection concentration (C_{Solution}) and stream concentration (C_{Stream}) (Equation 4.2.1.1).

$$Q_{\text{Tracer}} C_{\text{Tracer}} = Q_{\text{Solution}} C_{\text{Solution}} + Q_{\text{Stream}} C_{\text{Stream}} \quad 4.2.1.1$$

The conductivity sensors were compared to concentration of chloride in laboratory experiments. The relationship for reasonable tracer experiment values was linear with conductivity (Appendix, show figures from excel spreadsheet TRCR 7-30.xls).

4.2.2 Modeling for Stream Parameters

Analysis by OTIS-P (One-dimensional Transport In Streams – with Parameter estimation), a well-known model representing the one-dimensional advection and dispersion processes. This model is used to estimate storage zone parameters by statistically fitting a tracer experiment (Runkell, 1998; Harvey et al., 1996).

The transport processes that include any paths that retain flow contribute to transient storage. The transport processes and transient storage leave an imprint on the tracer signal through the stream. The tracer behavior can be modeled by a one-dimensional model of advection and dispersion (Equations 4.2.2.1 and 4.2.2.2) that includes a term for coupling the active channel with a transient storage zone (Bencala and Walters, 1983; Harvey et al., 1996). The tracer behavior in the main channel and in the

non-flowing storage zone where the flow is affected by four basic transport processes advection, dispersion, lateral flow, and storage zone exchange are represented by equations 14 and 15. This system was simplified in our study by selecting a site with no lateral surface inputs and the tracer molecule does not adhere to particles, or behave with sorption.

$$\frac{\partial C}{\partial t} = -\frac{Q}{A} \frac{\partial C}{\partial x} + \frac{1}{A} \frac{\partial}{\partial x} \left(AD \frac{\partial C}{\partial x} \right) + \alpha (C_s - C) \quad 4.2.2.1$$

$$\frac{dC_s}{dt} = \alpha \frac{A}{A_s} (C - C_s) \quad 4.2.2.2$$

The stream parameters are solved inversely from the concentration in the stream over time $\left(\frac{\partial C}{\partial t} \right)$; C , C_s are concentration in the stream and storage zones (we used specific conductivity). Some of the variables such as the volumetric flow rate of the stream (Q , $\text{m}^3 \text{s}^{-1}$) and stream distance (x) parallel to stream flow are measured directly during the tracer experiment. Others are solved within the parameter estimation program: D is longitudinal dispersion coefficient ($\text{m}^2 \text{s}^{-1}$), A and A_s are stream and storage-zone cross sectional areas, and α is the storage exchange rate (s^{-1}) (Bencala and Walters, 1983; Harvey et al., 1996; Harvey and Wagner, 2000; Runkell, 1998).

Using the storage parameters estimated by OTIS-P from the tracer experiments hyporheic flow is calculated as the product of the exchange rate and the cross-sectional area of the stream (equation 16, $\text{m}^3 \text{s}^{-1} \text{m}^{-1}$), assuming that all other processes in the stream contributing to transient storage are negligible (Harvey et al., 1996; Harvey and Wagner, 2000)

$$q_{hyp} = \alpha A$$

Wagner and Harvey (1997) systematically analyzed stream tracer study designs to improve methods for estimating parameters of rate-limited mass transfer. Wagner and Harvey (1997) found that in steep streams using a constant injection sampled through the rise, plateau and fall was able to provide more reliable parameter estimates than slug injections. Wagner and Harvey (1997) also found that using the Damkohler number (DaI) represented by equation x is a valuable indicator of the reliability of storage exchange parameter estimated (Bahr and Ruben, 1987).

A relationship between the Damkohler number (DaI) and the coefficient of variation of both the storage zone cross-sectional area (A_s) and stream-storage exchange coefficient (α) reveals that near a value of one for the Damkohler number ($DaI \approx 1$) both coefficient of variations are reduced (1997).

$$DaI = \frac{\alpha(1 + A/A_s)L}{v}$$

4.2.2 Hydrometric Measurements

Two piezometers were installed in the main channel to measure relative head between the stream and the substrate below the stream, with the purpose of measuring hyporheic flow. Two additional piezometers were installed in an ephemeral tributary channel that was dry down 60cm below the stream bed surface, and probably dry deeper, but a greater depth could not be attained. Installation of additional piezometers was planned, but the cobble dominated substrate and surrounding alluvium made installation extremely difficult. The piezometers were 3.8cm inside diameter pvc pipes, a 10cm

screened interval was cut into the pipe. The piezometers were inserted by driving a steel pipe with solid steel rod insert into the substrate, by removing the inner rod a piezometers could be inserted at desired depths. The two piezometers in dry tributary were driven down 60cm below substrate surface and did not reach water during the study period. The piezometer in the upper-riffle was driven down 30cm, where the top of the screened interval is at 20cm below stream/substrate contact. The piezometer in the upper-pool (reach length 10-meters) was driven down 35cm with the top of the screened interval at 25cm below the stream/substrate contact.

Hyporheic flow through a riffle-step-pool was calculated from the measurements at the piezometers as a two-dimensional hydraulic gradient (Equation 17) between the stream and substrate below the stream down to 30cm in order to check against values determined from the tracer technique. The hyporheic flow from the Darcy approach was approximated by

$$q_{hyp} = \frac{AK\left(\frac{\Delta h}{\Delta z}\right)}{L}$$

where A is the area of down-welling, K is the hydraulic conductivity determined from slug tests into piezometers (Appendix ?), $\Delta h/\Delta z$ is the hydraulic gradient between the stream and 30cm below stream bottom and is length between down-welling and up-welling morphologies. All down welling flow through the hyporheic zone is assumed to return despite loss to groundwater.

4.2.3 Temperature as a Tracer

The third method for measuring hyporheic flow uses the vertical temperature measurements through the substrate. Vertical temperature patterns are measured by

thermistor columns installed in x locations, locations are named from their relative location to the upstream boundary of the reach: 0-meter is a riffle, 10-meter is a pool, 15-meter is a pool-tail or riffle ... This method assumes that heat acts as a tracer as well. A daily pattern of temperature change can be seen in surface water. By observing the surface water temperature change in and how the timing of substrate temperature change is delayed a rate of advected flow can be estimated.

Temperature change with depth into the substrate was used as a tracer by assuming that the heat transfer is dominated by advection due to the high hydraulic conductivity and pore water velocities through the substrate. The velocity of the advected flow is calculated as the distance traveled vertically through the substrate (the distance between sensors) divided by the time of response for peak and minimum temperatures daily at depth (Figure).

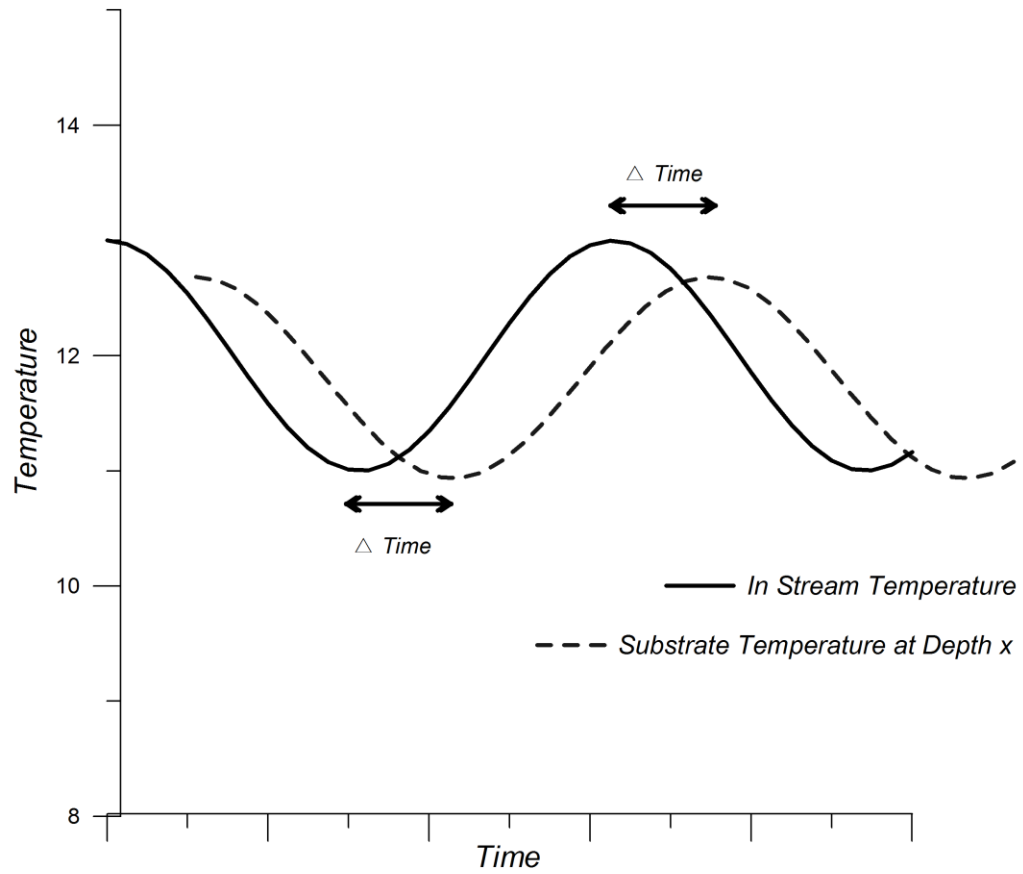


Figure 4.2.3. Conceptual graph showing time delay in daily temperature maximum and minimum from surface to arbitrary depth.

Hyporheic flow was calculated as travel time of the temperature peak to different distances and the ratio of heat conduction of the substrate (c_s) to water (c_w) (Constantz et al., 2003.)

$$q_{\text{hyporheic}} = \frac{V_t \left(\frac{c_s}{c_w} \right)}{L}$$

These rates were averaged over a ten-day period. The standard deviation of time to peak between the two locations was used to estimate the error of this measurement.

4.3 Results

4.3.1 Tracer Results

Tracer studies using a conservative chloride tracer were introduced into the stream to determine mean reach transient storage rates, used as a mean hyporheic advective water flow component for modeling temperature change over 100 to 200m reaches. The slug consisted of stream water with regular table salt dissolved in a bucket. To allow for mixing of the slug with the stream flow the slug was introduced well above the first point of interest. The results from the experiments discussed in this section are summarized in Table 4.3.1.

4.3.1.1 July 30,2003 Slug

This experiment was the only successful experiment during the study period. A couple of other attempts to measure breakthrough curves of tracers during the time period of the energy budget measurements failed. The reach length measured was ~60-meters from the boundary condition to the first sensor. An additional sensor farther downstream was not used because the tail of the tracer breakthrough curve was not recorded for this experiment. The breakthrough curve is matched well by the modeled results (Figure).

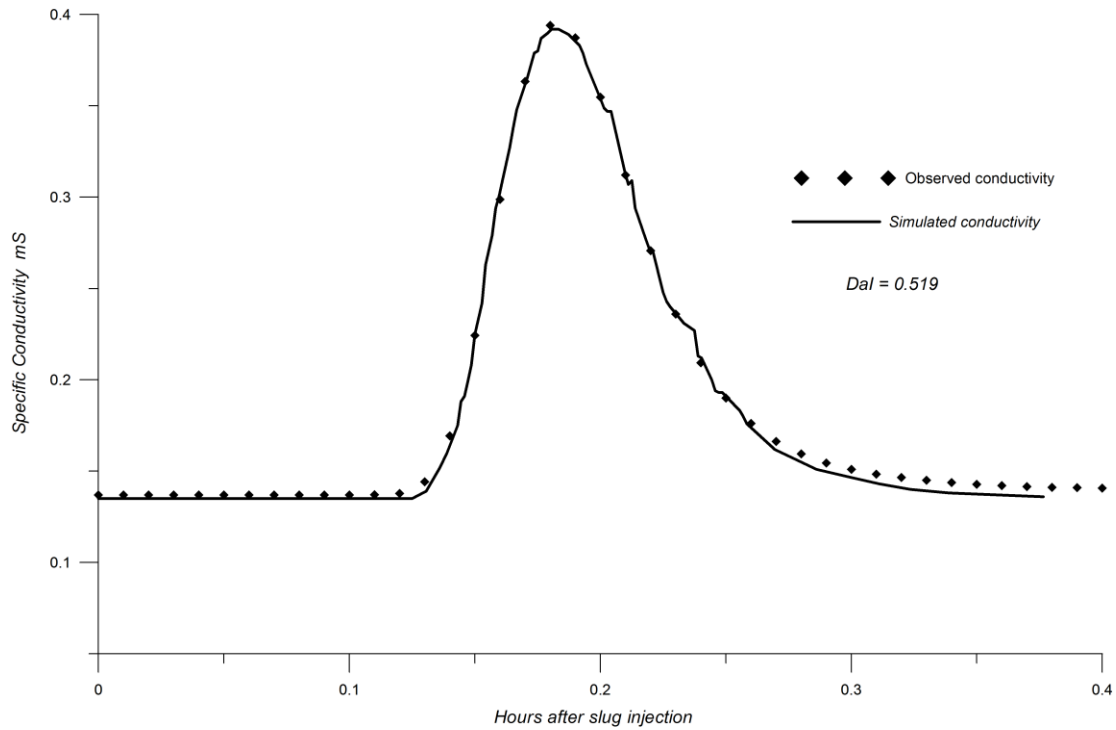


Figure x. Slug tracer breakthrough curve and model results.

The in-stream cross-sectional area was held constant during the modeling; the diffusion coefficient, storage zone cross-sectional area and the storage exchange rate were allowed to change during the modeling and parameter estimation processes. The calculated hyporheic flow (equation) resulted in a flow of $4.07\text{E-}5\text{m}^3\text{s}^{-1}$. The results for the stream parameters are summarized in Table 3.3.1.

4.3.1.2 June 4, 2004 Steady Injection

After reviewing literature about tracer design it was apparent that modeling steady injection tracers for stream parameters have a greater success rate. This experiment was conducted to check the parameter estimates and the hyporheic flow calculation against the slug method results from the prior summer. Although this experiment was a month earlier in the year the flow rate was similar to the preceding summer experiment.

Once again user malfunction reduced the efficiency of this experiment. The coupled tracer was not a complete failure due to the measurement of conductivity, but the fluorometer data was not recorded.

The breakthrough curve measured 500-meters downstream of the injection site shows a steep rising and falling limb with a plateau for approximately an hour. The simulated results do not match the plateau well but do line up well with the rising and falling limb. Although the estimated stream parameters were slightly different than the July 2003 slug tracer experiment the calculated hyporheic flow rate, from the two experiments, were on the same order of magnitude (Table 4.3.1). A slightly better Damkohler number (1.14) was calculated from the steady injection experiment.

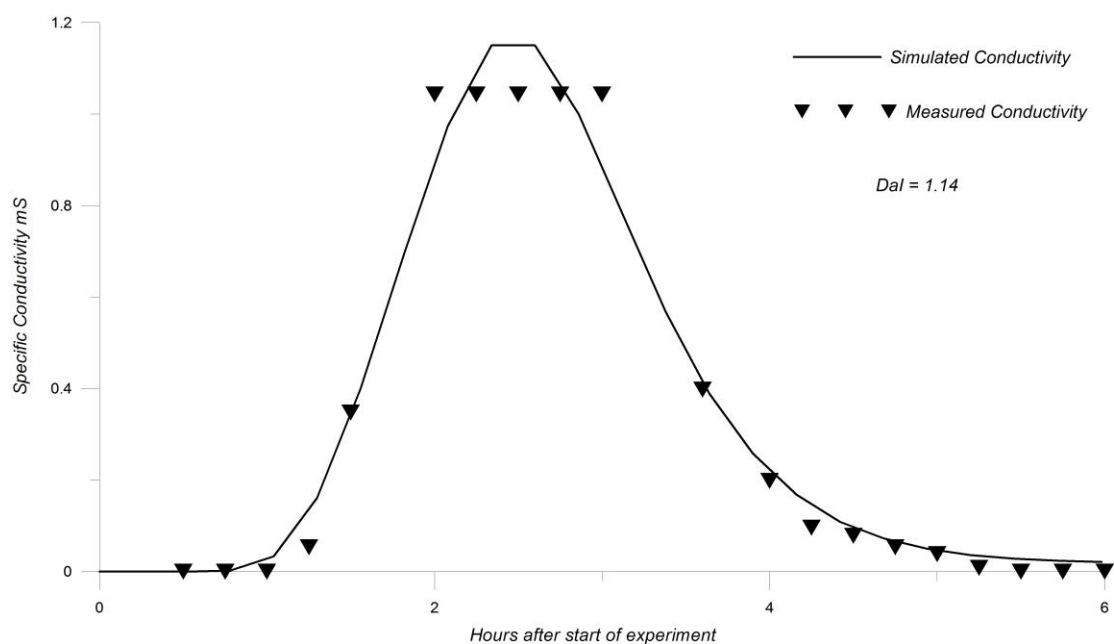


Figure x. Steady head injection break through curve and model simulation.

4.3.2 Hydrometric Results

The calculated hyporheic flow rate was determined from seven hydraulic head measurements. The hydraulic conductivity is $1 \times 10^{-4} \text{ m}^2 \text{ s}^{-1}$, measured from repeated slug tests in the piezometers in the pool and riffle (Appendix). The resulting calculated flow rate is $1.10 \times 10^{-5} \pm 2.89 \times 10^{-7} \text{ m}^3 \text{ s}^{-1} \text{ m}^{-1}$.

4.3.3 Vertical Temperature Profile Results

By observing the vertical temperature gradient through the substrate at the downwelling riffle (0-meter reach distance) the hyporheic flow rate is estimated for the same riffle and pool instrumented with the piezometers. This method does not rely on the absolute temperature measured but rather the timing of the temperature changes in the stream and how that timing compares with temperature changes in the substrate. We see a delay in the diurnal temperature variation at depth below the stream, for the purpose of estimating hyporheic flow we assume that the delay is related to the rate of water infiltration to depth from the surface. Although the value calculated by this method has a large error relative to the flow value, it is still on the same order of magnitude as the hydraulic head measurement calculations and the calculated value of hyporheic flow from the tracer experiments (Table 4.3.1).

Experiment Name	D	A	A _s	α	DaI	q_{hyp} $m^3 s^{-1} m^{-1}$
Piezometer Measurements, summer 2003	-	-	-	-	-	1.10E-5 ±2.89E-7
Slug tracer July, 2003	4.99	0.148	1.81E-2	2.75E-4	0.519	4.07E-5
Steady injection tracer June, 2004	2.04	0.148	1.81E-2	6.86E-5	1.14	1.02E-5
Vertical Temperature Profile in riffle	-	-	-	-	-	2.84E-5 ±1.33E-5

Table 4.3.1. A summary of calculated flow rates through the hyporheic zone (q_{hyp}) for the study reach and additional parameters if applicable to the method. D is a longitudinal dispersion coefficient, A is stream area, A_s is storage zone area, α is exchange rate and DaI is the Damkohler number.

4.4 Discussion

Tracer experiments are an excepted method for determining stream parameters, including hyporheic flow (Harvey et al., 1996; Harvey and Wagner, 2000), the weakness of the tracer experiment is in the assumptions that a majority of the transient storage is related to hyporheic flow. It is possible in most stream that have eddies and turbulent flow near steps into large pools that solute would be retained in surface features. Transient storage and hyporheic zone characteristics vary through a stream, using a tracer method should reveal a reach average value, the weakness of the tracer method is that the results reveal nothing about the processes involved in the transient storage or the hyporheic zone flow.

Kasahara and Wonzell (2003) showed that step-pool sequences caused exchange flows with relatively short residence times; using the flowrates and stream parameters the residence times can be calculated from the two tracer experiments by equation 4.4.1

(Harvey and Wagner, 2000). In this equation the relative areas between the stream and storage zone and the exchange rate are used.

$$t_s = \frac{A_s}{\alpha A}$$

The residence times were calculated to be ~7 minutes 25 seconds and 29 minutes 42 seconds for the slug and steady injection tracer respectively. There are large differences in these two times but both are short times, less than an hour. This is due to the short flow paths created by the stream morphology. The turnover length, L_s , or the distance required to route stream flow through the storage zones, hyporheic zone. This can be thought of as the distance traveled downstream by a parcel of water before entering the substrate (2000). The turnover length is calculated from the average in stream velocity, u , divided by the storage exchange coefficient estimated from the tracers (2000).

$$L_s = \frac{u}{\alpha}$$

The turnover lengths from the two tracers are calculated as ~760-meters and 3.8-kilometers for the slug and steady injection tracer respectively, using the average velocity measured during each experiment. Again a very wide range, but using the shorter and comparing to the reach length of 400-meters most of the water in the stream will have traveled through the storage zone by the time it reaches the downstream boundary.

4. Energy-Temperature Model and Model Evaluation

4.1 Introduction

The temperature changes were calculated as the change in stored heat energy per unit area divided by the volumetric heat capacity of water. Each of the components are measured or are calculated from environmental measurements.

To capture local meteorological variables a micro-meteorological station was installed ~30cm above the stream. All weather and temperature data was collected every 15 minutes. The weather station consisted of: a Kipp and Zonen CNR1 Net Radiometer to measure directional short and long-wave radiation 30cm above the stream. Wind speed measurements at two heights above the stream by R.M. Young Anemometer, both relative humidity and temperature were measured using a shielded HMP35C model temperature/relative humidity meter. The heat-temperature model in this study predicts a change in temperature for a defined reach length by measuring the change in stored surface heat energy for a parcel of water as it travels the reach length, determined by the average travel time for a parcel of water in the stream, dt .

The change in stored heat energy per unit area, $\Delta S/A$, is calculated as the flux of energy into or out of a unit area over time, Q_{total} (equation 1). A positive sign convention regarding heat transfer is into the stream. The temperature changes were calculated as the change in stored heat energy per unit area divided by the volumetric heat capacity of water (equation 2), $\rho_w C_w y$, where ρ_w is the density of water, C_w is the heat capacity of water and y is the average depth of the stream (Equation 3).

$$\frac{\Delta S}{A} = Q_{total} dt$$

$$\frac{\Delta S}{A} = C_w \rho_w y \Delta T$$

$$\Delta T = \frac{Q_{total} dt}{\rho_w C_w y}$$

The rate of heat flux in the system is attained by conservation of energy (Equation 4). A micro-meteorological station attained the meteorological variables necessary to close the heat budget approximately 30cm above the stream, the location of the station was selected to be typical of the study reach.

$$Q_{total} = Q_r + Q_{turbulent} + Q_{bed} + Q_{hyp} + Q_{gw} + Q_{friction} \quad (4)$$

Where Q_{total} is the sum of the components of the heat budget, (W/m^2). The rate of heat flux is calculated in fifteen-minute increments corresponding to the temperature and meteorological measurements.

Q_r	net radiation
$Q_{turbulent}$	combined turbulent fluxes: evaporation and sensible heat exchange
Q_{bed}	conduction with streambed
Q_{hyp}	heat flux associated with hyporheic flow
Q_{gw}	heat flux associated with groundwater flow
$Q_{friction}$	heat generated by friction

4.2 Methods

The following section describes the processes used to measure the hydrologic and the meteorological variables in the field during the study period. This section also describes the calculations of the specific heat budget components from the measured physical variables. A table of variables used in the following equations are provided in Appendix.

4.2.1 Net Radiation

The location of measurement of net radiation is assumed to represent a typical place along this reach. And although not quantified hemispherical photos taken from above the stream along the stream appear very similar to each other.

A Kipp and Zonen CNR1 Net Radiometer was used to measure directional short and long-wave radiation 30cm above the stream. The radiometer was under the canopy, so periodically direct sunlight would penetrate the canopy and be recorded as a spike in the data when most of the stream was still shaded; by averaging over five time steps the radiation data is smoothed with for a decrease in violent changes in radiation values.

4.2.2 Turbulent Energy Fluxes

Q_s and Q_e are the turbulent fluxes associated with sensible heat and latent heat exchange from evaporation. The Penman or combination equation was used to determine the heat component associated with evaporation only from free-water surface, Q_e (Equation 5) not including loss of water from the channel through transpiration.

$$Q_E = \frac{\Delta(K + L) + \gamma K_E \rho_w \lambda_v v_a e_a^* (1 - W_a)}{(\Delta + \gamma)}$$

where Δ is the slope of the relationship between saturation vapor pressure and temperature, K is solar radiation, L is longwave radiation, γ is the psychrometric constant (equation 6 and 7), K_E is a coefficient that represents the efficiency of vertical transport of water (equation 8), ρ_w is the density of water, λ_v the latent heat of vaporization that decreases with increase of temperature of the evaporating surface, v_a is the wind speed measured one-meter above the stream surface, z_m , measured by a **R.M. Young Anemometer**, z_d is the zero-plane displacement and z_0 is the roughness height of the surface, e_a^* is the saturation vapor pressure of air, and W_a is the relative humidity of the air and T_a is air temperature both measured by a shielded HMP35C model temperature/relative humidity meter (Dingman, 2002). We used a typical constant value of 101.3kPa for pressure, P .

$$\gamma = \frac{c_a P}{0.622 \lambda_v}$$

$$\Delta = \frac{2508.3}{(T + 237.3)^2} * \exp\left(\frac{17.3T}{T + 237.3}\right)$$

$$K_E = \frac{0.622 \rho_a}{P \rho_w} * \frac{1}{6.25 \left[\ln\left(\frac{z_m - z_d}{z_0}\right) \right]^2}$$

The heat associated with sensible heat, Q_s , was determined by rearranging the Bowen ratio (Equation 9). The Bowen Ratio depends on the surface and air temperatures (T_s , T_a) and vapor pressures (e_s , e_a) and the psychrometric? constant (γ , Equation 6).

$$Q_s = \gamma \left(\frac{T_s - T_a}{e_s - e_a} \right) Q_e$$

4.2.3 Bed Conduction

Q_{bed} is the heat flux from bed-conduction calculated from vertical temperature gradient through the substrate measured by thermistor columns (Equation 6) and corrected for radiation absorbed through the bed (Equation 7) (Webb and Zhang, 1997).

$$Q_{bed} = K T_g - R_{ad}$$

$$R_{ad} = (1 - a)(1 - r)(1 - d) Q_r e^{-fy}$$

Where K is the thermal conductivity of the substrate, T_g is the thermal gradient in the substrate, R_{ad} is the radiation absorbed by the bed calculated by equation 11, where a is albedo, r is fraction absorbed in water layer, d is fraction reflected by stream bed, f is the attenuation coefficient and y is water depth.

4.2.4 Hyporheic Energy Component

The heat budget component associated with advected water through the hyporheic zone, Q_{hyp} , uses the measured difference between down-welling stream temperature (T_s) measure at the stream/substrate interface in a riffle and upwelling return flow temperature (T_{hyp}) measured in the pool at 5-centimeters depth below the stream/substrate interface, volumetric heat capacity of water $C_w\rho_w$, mean stream width (w) and the exchange rate with the hyporheic zone (q_{hyp}) (Equation).

$$Q_{hyp} = \frac{C_w\rho_w q_{hyp} (T_s - T_{hyp})}{w}$$

4.2.5 Friction

Although fluid friction, $Q_{friction}$, is negligible small relative to other heat components and in most studies of stream temperature modeling is not included, the component is calculate to show the comparison in this steep stream. Fluid friction was calculated by

$$Q_{friction} = 9805(q_{stream}/W)S$$

where the only changing variable is stream flow(q_{stream}), slope (S) and channel width (W) were constants (Reference ?).

4.3 Results

The weather during the study period was dry with no recorded or observed rainfall. Instrumentation was installed in mid July and all equipment was working well during the study period. The first four days of the study period had similar high and low temperatures but the last couple days of the study the high temperatures were much lower.

4.3.1 Energy Components

The energy components described in this section are shown for a six-day period where all instruments meteorological, hydraulic and temperature were recording (Figure 4.3.1).

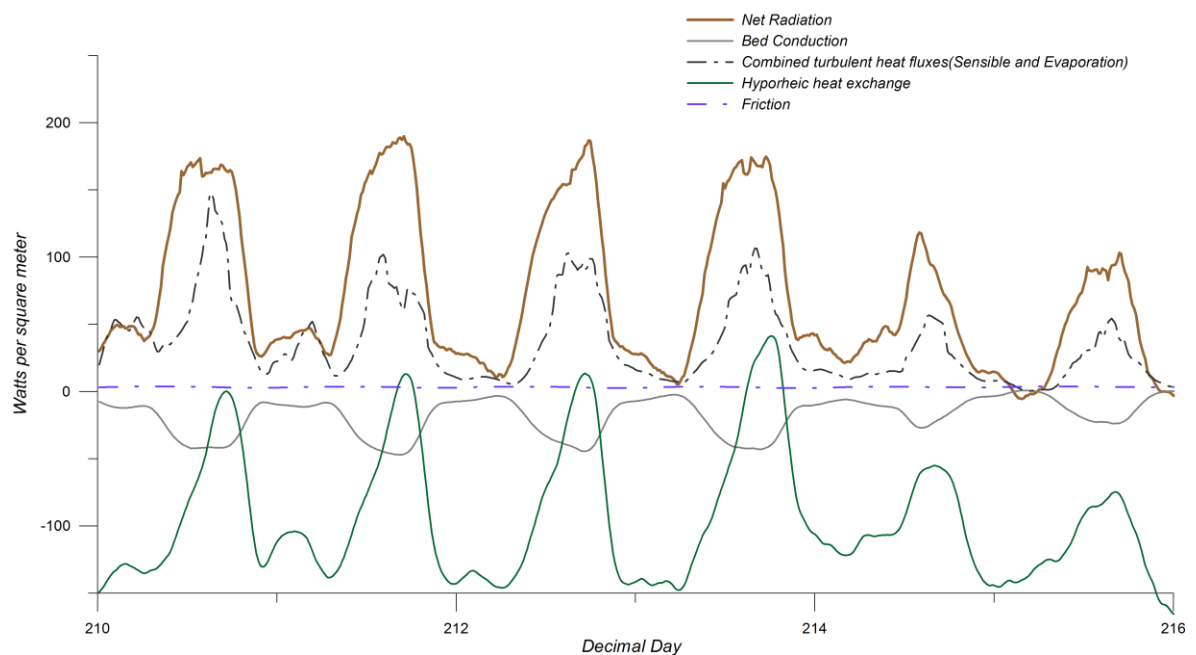


Figure 4.3.1. Heat energy components during the study period.

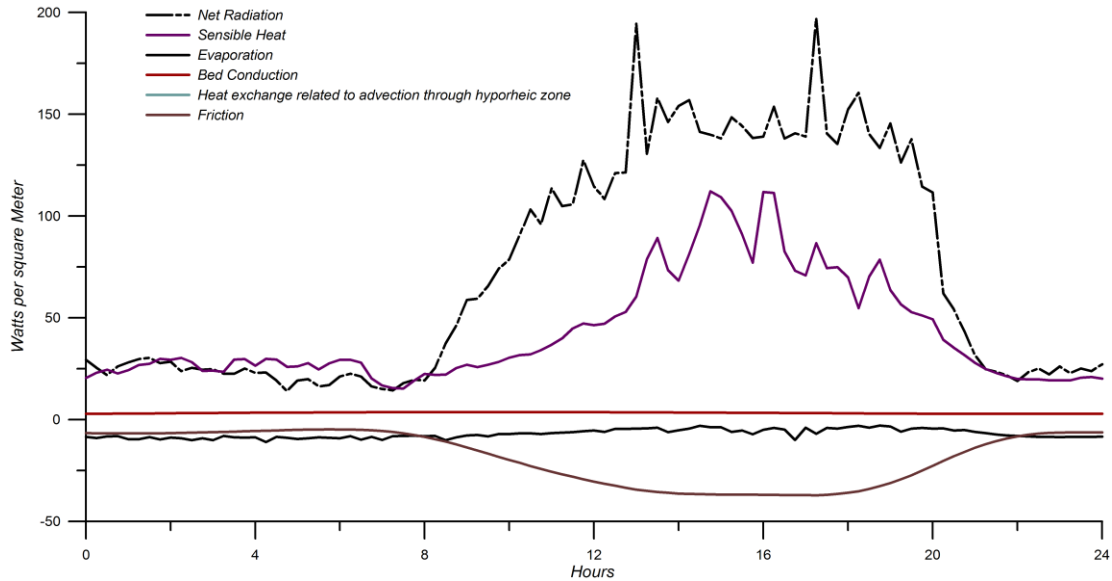


Figure 4.3.2. Averaged daily heat energy components.

Turbulent heat flux components calculated from measured air temperature, relative humidity and wind speed (equation) varied slightly each day (Figure). The daily loss of energy from latent heat from evaporation was much smaller than the gain from the sensible heat exchange with the atmosphere (24-hour average figure). The calculated evaporative flux includes only the evaporation directly from the water surface, it does not take into account transpiration from the trees which has little direct effect on stream temperature. The two terms Latent Heat Exchange from Evaporation and Sensible Heat Exchange with the atmosphere are combined in the heat budget as the Turbulent Heat Exchange component (Figure).

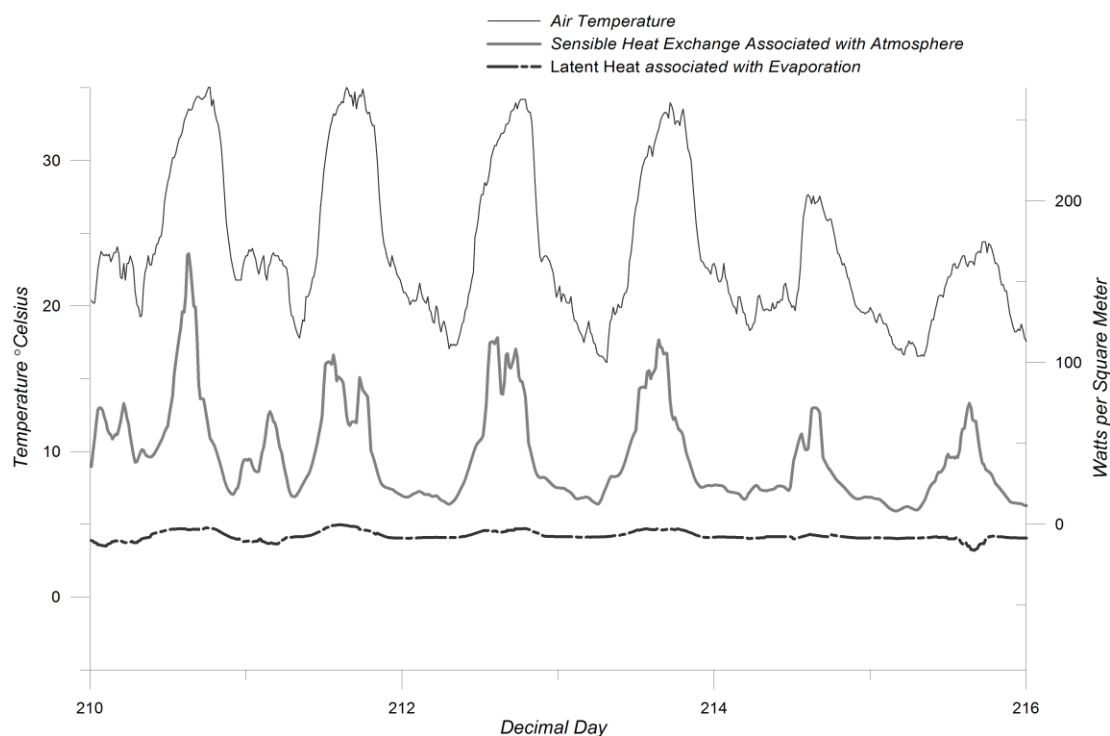


Figure 4.3.1. Turbulent heat flux components. Daily sensible heat exchange and latent heat exchange associated with evaporation. Notice the dependence of the sensible exchange on air temperature.

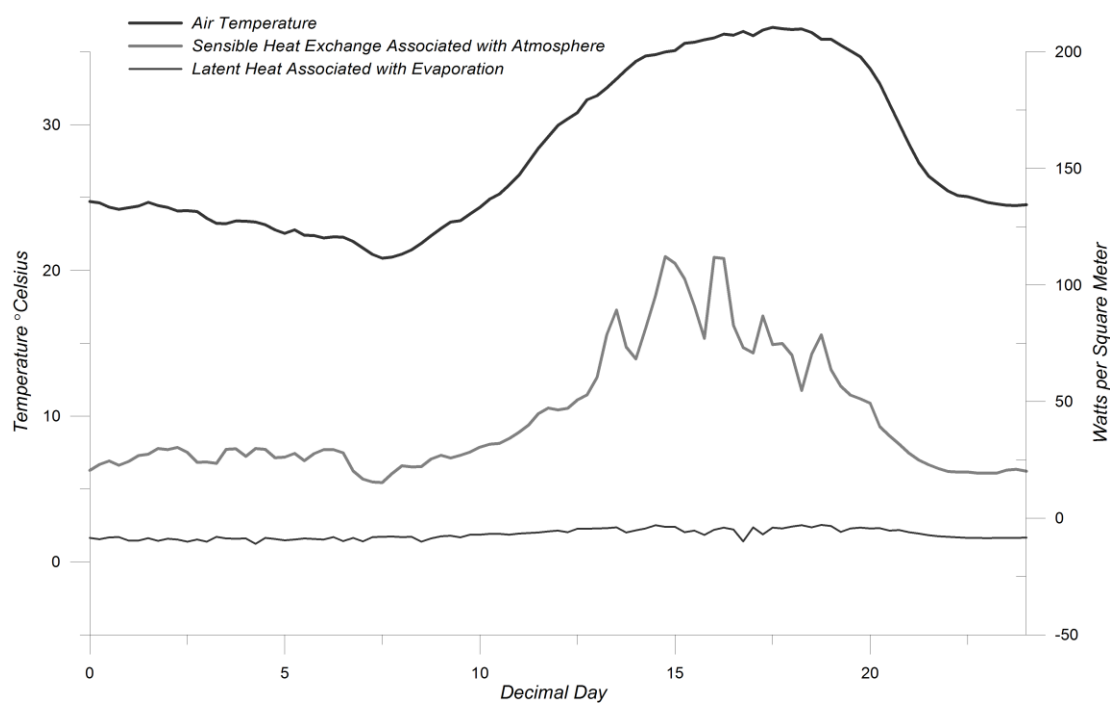


Figure 4.3.2. Daily averaged turbulent heat flux components during the study period.

<u>Component</u>	<u>Average Daily Flux Into System</u>	<u>%</u>	<u>Average Daily Flux Out of System</u>	<u>%</u>
Net Radiation	42191.37	63.01%	-98.29	0.20%
Sensible Heat	24745.40	36.95%	0.00	0.00%
Evaporation	0.00	0.00%	-4311.01	8.87%
Bed Conduction	0.00	0.00%	-10679.95	21.98%
Hyporheic Heat Exchange	0.00	0.00%	-33508.80	68.95%
Friction	4.68	0.01%	0.00	0.00%

Table 4.3.2. Summary of cumulative heat energy fluxes, averaged daily over the study period.

4.3.2 Model Results Compared to Measured Temperature Change

This section uses the results from the measured and calculated energy components shown in the previous section of this chapter. The components of the heat budget are combined conservatively (Equation) resulting in a net flux of energy flow into or out of the stream per time, and a change in temperature (Equation). This time series data is used with the temperature change measurements to assess the influence of the budget components on stream temperature.

The 20-meter model of temperature change versus the measured temperature change does match well during the time period associated with rising and falling temperatures but does not fit the peak temperature time of day; the model predicts a greater magnitude of temperature increase. All values used in the model are reach average values, the heterogeneity of the heat energy component associated with hyporheic flow has a reach length on the order of the stream morphologic features, the spacing of the pools. The reach average values for some energy components may miss represent the actual local energy flux rates, resulting in an inaccurate temperature change prediction. In the case of the 20-meter reach prediction, I believe that the hyporheic flow in actuality has a greater affect than the model predicts, due to the use of reach average

values. The idea of localized temperature change and stream temperature heterogeneity is important to consider, it supports the knowledge that local cooling is associated with stream morphologic features where return flow from the substrate occurs. This idea is supported by the longitudinal temperature patterns recorded, showing a general downstream increase in temperature, but some local cooling associated with pools (Figure x and y). When the hyporheic energy component is excluded from the heat budget to predict temperature change the basic daily trends and timing of heating and cooling match the measured, but the model over predicts at all times of the day; the hyporheic flow contributes a cooling or a buffer to the heating of stream waters daily at a reach scale of 20-meters.

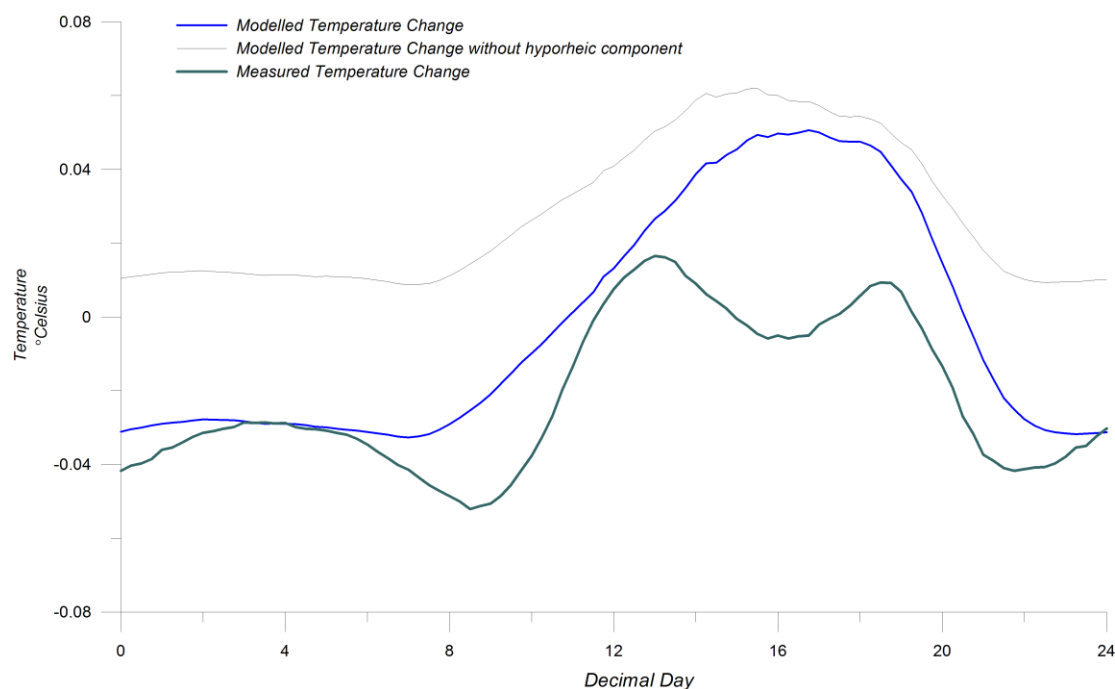


Figure 4.3.4. Measured and modeled temperature change for the first 40-meters of the study reach. The predicted temperature change is shown including and excluding the hyporheic exchange energy component.

The prediction of temperature change for the 400-meter reach length does fits the daily patterns of heating and cooling well. The timing of the temperature increase and the peak are better fit at this longer stream length. The falling limb does not match as accurately. The model predicts a greater magnitude of temperature increase with and without the hyporheic energy component included. All values used in the model are reach average values, the heterogeneity of the heat energy component associated with hyporheic flow has a reach length on the order of the stream morphologic features, the spacing of the pools.

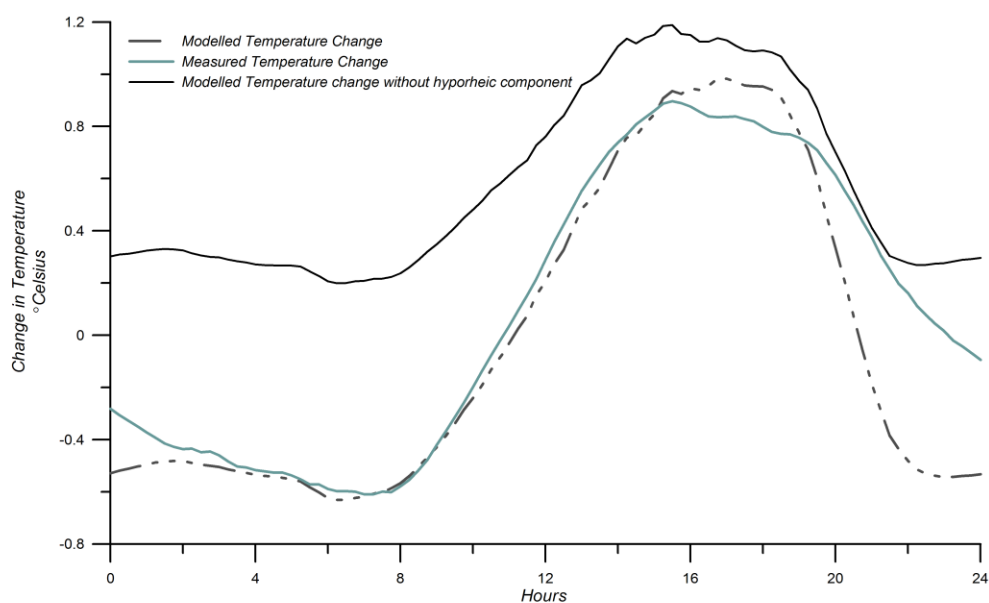


Figure 4.3.5. Measured and modeled results for an average 24-hour period of temperature change for the 400-meter reach distance.

Summarize results again. The heat budget with the hyporheic flow fit the downstream temperature changes more closely than the model excluding the heat component associated with hyporheic flow. With the hyporheic heat component the most important energy inputs to the stream daily were net radiation and sensible heat transfer from the atmosphere at 63% and 37% respectively, the only two significant inputs. The most important heat components out of the stream were

During the field campaign the stream maintained a typical flow of $0.01\text{m}^3/\text{s}$ and was steadily losing flow to the subsurface, with some flow returning through hyporheic exchange. Under different hydrologic circumstances the relative importance of each flux may vary greatly. For example in a system where the stream is gaining flow from groundwater hyporheic flow would be subdued and groundwater would control stream temperature. Although the results from the heat budget may be limited to very similar circumstances and stream type, these are the dominant conditions for streams in the semiarid western United States, where head water streams have a minimum stream flow during summers often going dry and losing to groundwater.

Some specific problems with the heat budget lie in the measurement and calculation of specific components. In addition to over predicting hyporheic flow using the tracer method we recognize that the component of heat transfer from hyporheic flow is closely related to bed conduction and that it is possible that each may be under appreciated or over accounted for. An additional observation about hyporheic fluxes and groundwater is that hyporheic flow may decrease at night due to the increase in shallow groundwater fluxes when plant transpiration decreases. This has implications for

situations where trees are clear-cut around a stream in addition to the obvious radiation/shading effects.

Evaporative flux calculated was less than expected in other studies (Webb and Zhang, 1997 and 1999) evaporation was a dominant cooling component in the budget. This may be a unique characteristic of steep headwater streams and is probably due to the sheltered nature of the stream documented by the wind speeds measurements. The channel where the weather station was installed is near a steep hill slope on the south side and has gullied slightly having a steep bank/flood plain on the north side. The channel is typically very confined in a narrow canyon with steep hill slopes to either side, and roughness from vegetation around and above the stream surely shelters the stream from much wind.

The importance of each energy flux is determine for this study reach, as Webb and Zhyang (1997) notes the energy fluxes can vary widely in magnitude and significance depending on local stream characteristics, time of year and weather patterns. Despite this I believe that this study reveals a good quantitative and conceptual relationship between dominant heat energy fluxes and stream temperature for not only this stream but countless other small headwater streams in the semiarid climate of the western United States.

5 CONCLUSIONS

The overall goals of this study were to accurately predict longitudinal temperature change in stream waters by using a heat budget model and to evaluate the impact of heat

energy fluxes on stream temperature specifically hyporheic flow in an energy budget approach to predict downstream changes in stream temperature.

Results from section 2 demonstrate that stream temperature generally increases down stream, but with some local heterogeneity as a morphologic scale. Where zones of up welling, specifically the pools buffer the over all down stream warming trend.

In Section 3 hyporheic flow was specifically examined by several methods. One method uses the temperature measurements from section 2, the vertical temperature profiles show attenuated heating from the surface in down welling zones and more of a homogeneous temperature profile in the up welling zones. The hyporheic flow, driven by the stream morphology and gradient, has a short residence time and short flow paths, on the order of reach morphology. The turnover length, or the average longitudinal stream distance a parcel of water travels before entering the storage zone, or in our study assuming that all of the storage zone is the hyporheic zone, is only 300 to 400 meters longer than the total study reach length. The calculations of hyporheic flow and residence time support the assumption that short but frequent flow through the substrate may influence stream temperature, leading to the next section where stream temperature is examined in more detail. To examine the question of stream temperature and the importance of the hyporheic zone a heat energy budget is used to compare the effects of major heat fluxes and stream temperature.

Section 4 shows that net radiation and sensible heat from the air are the highest contributing heat energy fluxes during the low flow summer months. During these months the low may also relate to the highest relative effects from hyporheic flow. The

low flow summer also is the highest period of air temperature, thus the high sensible heat flux to the stream.

To understand more try different systems. Controlled flow situations where diversions and inputs are known.

Discussion of possible management uses for this model, at least conceptually you know what sources would increase and decrease with land use...

REFERENCE

- Bencala, K.E. and R. A. Walters, 1983. Simulation of solute transport in a mountain pool-and-riffle system: A transient storage model. *Water Resources Research* 19: 718-724.
- Brown, G.W. 1969. Predicting temperatures of small streams. *Water Resources Research*. 5,68-75.
- Buffington, J.M., and D.R. Montgomery, 1999, A procedure for classifying textural facies in gravel-bed rivers, *Water Resources Research*, 35, (6), 1903-1914. maybe don't need
- Campbell Scientific, 2002, CR10X Measurement and Control Module Operator's Manual, Revision 1/02, Section 9 and 13.
- Constantz, J. Tyler, S.W. and Kwicklis, E., 2003, Temperature-Profile Methods for Estimating Percolation Rates in Arid Environments, *Vadose Zone Journal*, 2: 12-24.
- Constantz, J., Stewart, A.E., Niswonger, R., and Sarma, L., 2002, Analysis of temperature profiles for investigating stream losses beneath ephemeral channels, *Water Resources Research*, in press.
- Franken, R.J.M., R.G. Storey and D..D.Williams, 2001, Biological, chemical and physical characteristics of downwelling and upwelling zones in the hyporheic zone of a north-temperature stream. *Hydrobiologia* 444: 183-195.

Harvey, J.W., B.J. Wagner, and K.E. Bencala. 1996. Evaluating the reliability of the stream tracer approach to characterize stream-subsurface water exchange. *Water Resources Research* 32:2441-2451.

Harvey, J.W. and B.J. Wagner, 2000, Quantifying Hydrologic Interactions between streams and their subsurface hyporheic zones: book chapter in *Streams and Ground Waters*, eds. Jones J.B. and Mulholland, P.J., Academic Press: 4-41.

Kasahara, T., and Wonzell, S.M., 2003, Geomorphic Controls on Hyporheic Exchange Flow in Mountain Streams. *Water Resources Research*, 39, (1).

McKee, J.E., and H.W. Wolf, 1963, *Water Quality Criteria*. Second Edition, Sacramento Calif., p.548.

Montgomery, D.R., and Buffington, J.M., 1997, channel-reach Morphology in Mountain Drainage Basins, *Geol. Soc. Am. Bull.*, 109, 596-611.

Moore, R.D. and Sutherland, P.W., 2002, Thermal Processes and Temperature Patterns in a Complex Headwater Stream Within a Clear *Eos Trans. AGU*, 83(47), Fall Meet. Suppl., Abstract H52A-0843.

Mulholland, P.J., and D.L. DeAngelis, 2000, Surface-Subsurface Exchange and Nutrient Spiraling: book chapter in *Streams and Ground Waters*, eds. Jones J.B. and Mulholland, P.J., Academic Press: 149-166

Pringle, C.M., and F.J. Triska, 2000, Emergent Biological Patterns and Surface-Subsurface Interactions at Landscape Scales: book chapter in *Streams and Ground Waters*, eds. Jones J.B. and Mulholland, P.J., Academic Press: 167-193.

- Rucker, R.R., B.J. Earp, and E.J. Ordal, 1953. Infectious Diseases of Pacific Salmon. Transactions of the American Fisheries Society 83, 297-312.
- Runkell, R.L., 1998. One-dimensional transport with inflow and storage (OTIS): A solute transport model for streams and rivers. *Water-Resources Investigations (U.S. Geological Survey)*, Report 98-4018.
- Silliman, S.E., and Booth, D.F., 1993, Analysis of time-series measurements of sediment temperature for identification of gaining vs. losing portions of Juday Creek, Indiana: Journal of Hydrology, v.146, p.131-148.
- Story, A., Moore, R.D. and Macdonald, J.S., 2003, Stream Temperatures in two Shaded Reaches Below Cutblocks and Logging roads: Downstream Cooling Linked to Subsurface Hydrology, Can. J. For. Res./Rev. Can. Rech. For. 33(8): 1383-1396.
- Wagner, B.J., and J.W. Harvey, 1997. Experimental design for estimating parameters of rate limited mass transfer: Analysis of stream tracer studies. *Water Resources Research* 33: 1731-1741.
- Webb, B.W. and Y. Zhang. 1997. Spatial and seasonal variability in the components of the river heat budget. *Hydrological. Processes.* 11,79-101.
- Webb, B.W. and Y. Zhang, 1999. Water temperatures and heat budgets in Dorset chalk water courses. *Hydrological Processes* 13: 309-321.

APPENDIX A Tracer Method stuff and otis-p

Otis outline and transient storage estimation

Assumptions with otis, solute concentration varies only in the longitudinal direction. Using conservation of mass and breaking each stream segment into two parts, the main channel and the storage zone the exchange is determined by a first order mass transfer process for a conservative tracer.

Other assumptions (p. 6).

Main Channel

The physical processes affecting solute concentration are advection, dispersion, lateral flow and transient pool storage. I am assuming that there is no lateral exchange, so that the only physical processes that are considered are advection, dispersion and transient storage.

The chemical reactions affecting solute concentration include sorption to the streambed and first-order decay, I am using a chloride tracer and assuming that it is conservative.

All model parameters describing physical processes and chemical reactions may be spatially variable.

Model parameters describing advection and may be temporally variable. These parameters include volumetric flow rate, main channel cross-sectional area. All others are temporally constant.

Storage zone

Advection, dispersion, lateral flow does not occur in the storage zone.

I am assuming no sorption or decay.

All model parameters describing transient storage and chemical reactions may be spatially variable.

All model parameters describing transient storage and chemical reactions are temporally constant.

Parameter estimator

mean	A	main channel cross-sectional area (L^2)	assuming constant, using
	A_s	storage zone cross-sectional area (L^2)	estimated
	C	main channel solute concentration (M/L^3)	measured

C_L	lateral inflow solute concentration	controlled/assumed none
D	dispersion coefficient (L^2/T)	estimated
Q	volumetric flow rate (L^3/T)	invariable
α	storage zone exchange coefficient ($/T$)	estimated
x	distance	
t	time	

The one-dimensional model of advection and dispersion in streams includes terms for the active channel and for storage zones, and is simulated as a mass transfer between the stream and storage reservoirs. By assuming no lateral flow the main channel and storage-zone mass balance are described by the coupled differential equations 7 and 8.

$$\frac{\partial C}{\partial t} = -\frac{Q}{A} \frac{\partial C}{\partial x} + \frac{1}{A} \frac{\partial}{\partial x} \left(AD \frac{\partial C}{\partial x} \right) + \alpha (C_s - C)$$

$$\frac{dC_s}{dt} = \alpha \frac{A}{A_s} (C - C_s)$$

By modeling the stream tracer concentration, C , the mean characteristics for transient storage, the exchange coefficient α (T^{-1}), storage zone cross-sectional area A_s , and storage zone tracer concentration C_s can be determined for the modeled reach. In stream variables: longitudinal dispersion coefficient, D , main channel cross-sectional area, A , and the volumetric in stream flow rate, Q , are also either estimated by the model or measured in the field.

APPENDIX B

datalogger work, wiring and devices

APPENDIX C constants and values used in energy budget, table form with some description as well.

data or tables ? necessary?

Field Methods (Figure: Field diagram illustrating instrument set-up)

During the summer field campaign routine maintenance was conducted almost daily, including downloads of the weather station and temperature data. Much of the field season was spent adjusting instrumentation to record all necessary measurements simultaneously.

Turbulent Heat Budget Component Constants

ρ_{atm}	1.25 Kgm ⁻²	Density of atmosphere
P	101.3 kPa	Atmospheric pressure
C_a	0.025 MJkg ⁻¹	Heat capacity of the atmosphere
z_m	0.5 m	Instrument height above stream
z_o	0.05 m	Roughness height of stream surface
z_d	0.001 m	Zero plane displacement of stream surface
K_H	3.76E-5 MJ (mK) ⁻¹	Bulk Sensible-heat transfer coefficient
v_a	ms ⁻¹ measured	Wind speed

Bed Conduction Heat Component Constants

a	0.1	Albedo of water surface
r	0.65	Fraction of radiation absorbed in water surface layer
d	0.2	Fraction of radiation reflected by stream bed surface
f	0.05 m ⁻¹	
y	0.19 m	Mean stream depth